

# Going Deeper with Spectral Embeddings

Vivien Cabannes

June 2, 2023

## Abstract

To make sense of millions of raw data and represent them efficiently, practitioners rely on representation learning. Recently, deep connections have been shown between these approaches and the spectral decompositions of some underlying operators. Historically, explicit spectral embeddings were built from graphs constructed on top of the data. In contrast, we propose two new methods to build spectral embeddings: one based on functional analysis principles and kernel methods, which leads to algorithms with theoretical guarantees, and the other based on deep networks trained to optimize principled variational losses, which yield practically efficient algorithms. Furthermore, we provide a new sampling algorithm that leverages learned representations to generate new samples in a single step.

## 1 Introduction

A long-standing problem in artificial intelligence has been to extract good features from raw data that, once fed to supervised learning algorithms, would ease the learning process. For example, images can be stored as arrays of pixels stored in computer memory, but learning to recognize patterns or segment objects based on these raw data is quite challenging. Historically, features were manually engineered using domain-expert knowledge. However, with the advent of larger datasets and the increase of computing resources, generic methods have emerged to process large amounts of data, deduce a structure beyond them, and design new embeddings of the data.

From a mathematical standpoint, many representation learning algorithms can be seen as estimating the eigenfunctions of some base operators. Embeddings that are linked to the spectral decomposition of an operator are known as spectral embeddings. In the machine learning literature, spectral embeddings are often understood thanks to graph theory as the eigenvectors of some graph built on top of the data. However, we will argue that a richer picture can be offered by functional analysis perspectives that drop out graph theory. Our contributions are two-fold.

1. Firstly, we recall how certain operators, if approximated properly, can be used to efficiently embed input data (i.e. “solve” representation learning). Additionally, we introduce a new “pushforward sampler” that leverages those embeddings to generate plausible new data (i.e. “solve” some aspect of generative AI).
2. Secondly, we present principles for estimating these operators and provide two procedures to approximate them. One approach is based on neural networks and generalizes recent algorithms that are empirically effective. The other approach is based on kernel methods and generalizes recent algorithms that offer theoretically guarantees. For this kernel approach, we derive two algorithms to use Laplacian regularization, with a number of floating point operations comparable to that of the Nyström method. This derivation enables the future use of derivatives in kernel regression essentially for free.

The prototypical example of spectral embedding is given by a Laplacian operator. Laplacians are helpful for representation learning as they encode some sort of “modes” on the input space, together with a notion of complexity of those (e.g. think of Fourier modes where complexity increases with frequency). They are also used in generative AI (that aims to generate new samples that look like the original data) as they describe Langevin diffusion dynamics toward any specified stationary measure.

Overall, this paper offers efficient algorithms and a principled framework to estimate spectral embeddings, and unveils new links between diffusion models and representation learning.

**Related work.** The usefulness of Laplacian spectral embeddings for representation learning has been discussed extensively over the last two decades. Laplacians were introduced in the realm of computer science through graph-Laplacian (Chung, 1997), and were integrated soon after into machine learning (Zhu et al., 2003; Belkin and Niyogi, 2003), before theory was derived regarding their convergence towards real Laplacian operators (Hein et al., 2007; Singer, 2006). Recently, new insights were provided by Cabannes et al. (2021); Pillaud-Vivien and Bach (2023). This serves as a strong inspiration for Algorithm 4. In this meantime, deep learning practitioners have developed similar ideas, beginning with the TangentProp algorithm of Simard et al. (1991). This stream of research has led to self-supervised learning methods that have become the state-of-the-art for representation learning (Chen et al., 2020; Zbontar et al., 2021; Bardes et al., 2022). Recent works have cast deep links between those new methods and spectral embedding (HaoChen et al., 2021; Balestrieri and LeCun, 2022). This serves as a strong inspiration for Algorithm 3, which can be seen as generalizing recent ideas in the physics community (Zhang et al., 2022).

Laplacian operators are also known as the generators of the overdamped Langevin dynamics, which can be used as a diffusion process for sampling (see e.g. Bakry et al., 2014). Discretizing the diffusion leads to the Langevin Monte Carlo or Metropolis-adjusted Langevin algorithm (Grenander and Miller, 1994; Roberts and Tweedie, 1996; Andrieu et al., 2003), which has been used to generate samples given access to an unnormalized density (see e.g. Chewi, 2023). In machine learning, the picture is quite different, as the goal is to generate fresh samples that look like previous examples. However, recent advances have shown the usefulness of diffusion models in those generative settings (e.g. Ho et al., 2022; Rombach et al., 2022), notably when accessing their infinitesimal generators (Liu and Wang, 2016). Reciprocally, diffusion processes can be used to compute spectral embedding in a power method fashion (Han et al., 2020). The “pushforward sampler” approach considered here was not directly inspired by any of those papers, but derived from scratch based on simple theoretical observations for SDE.

## 2 Why do spectral embeddings matter?

This section reminds the reader of the concept of spectral embedding, introduces an illustrative Laplacian operator, and explains its usefulness for representation learning and for sampling.

### 2.1 Definition and examples

Machine learning settings start with some data that are assumed to have been collected and stored as raw vectors  $x \in \mathcal{X} = \mathbb{R}^d$ , which will be used as inputs for computer programs. The collection process is idealized as underlying a distribution  $\rho \in \Delta_{\mathcal{X}}$  which generates  $n$  independent variables  $(X_i) \sim \rho^{\otimes n}$ , i.e.  $n$  input samples. Spectral embeddings consist in defining embeddings  $\varphi : \mathcal{X} \rightarrow \mathbb{R}^m$ , or representation of the data, based on the spectral decomposition of an operator  $\mathcal{L}$  on  $L^2(\rho)$ , could it be its eigen or its singular value decomposition. E.g., if a positive symmetric operator  $\mathcal{L}$  is diagonalized in  $L^2(\rho)$  as

$$\mathcal{L} = \sum_{i \in \mathbb{N}} \lambda_i f_i \otimes f_i, \quad (1)$$

for  $\lambda_i > 0$  the eigenvalues of  $\mathcal{L}$  sorted in increasing order and  $f_i \in L^2(\rho)$  the corresponding eigenfunctions, those embeddings could be (see e.g. Coifman and Lafon, 2006; Cabannes et al., 2023b)

$$\varphi_{\text{diff.maps}} = (\exp(-\beta \lambda_i) f_i)_{i \in [m]}, \quad \varphi_{\text{VICReg}} = (\sqrt{(1 - \beta \lambda_i)_+} f_i)_{i \in [m]}, \quad (2)$$

for some parameter  $\beta > 0$  that assimilates to an inverse temperature.

**The Laplacian example.** To ground the discussion, a prototypical example is provided by a Laplacian operator. The Laplace operator, also known as Laplacian, is arguably the most natural differential symmetric operator. It is defined as the sum of unmixed second-order partial derivatives. Equivalently,

it is characterized as the divergence of the gradient; the divergence being itself characterized as the adjoint of the gradient. Those two observations unveil generalizations of the Laplace operator into a rich family of operators also named Laplacians. Laplacians are differentiated by two factors: the geometry to define adjunction, the manifold to define gradients. Those operators describe many physical phenomena, such as heat diffusion, relations between electrostatic (resp. gravitational) potentials and charge (resp. mass) distributions, or wave equations. The running example of this study will be the Laplacian  $\mathcal{L} = \nabla^* \nabla$  where  $\nabla$  is the Euclidean gradient, and the adjoint is taken with respect to the  $L^2(\rho)$  geometry.<sup>1</sup> In other terms,  $\mathcal{L} : L^2(\rho) \rightarrow L^2(\rho)$  is defined for  $f$  and  $g$  in  $L^2(\rho)$  as

$$\langle f, \mathcal{L}g \rangle_{L^2(\rho)} = \mathbb{E}[\langle \nabla f(X), \nabla g(X) \rangle]. \quad (3)$$

The quadratic form associated with  $\mathcal{L}$  is known as the Dirichlet energy, it reads

$$\mathcal{E}_{\mathcal{L}}(f) = \langle f, \mathcal{L}f \rangle_{L^2(\rho)} = \mathbb{E}[\|\nabla f(X)\|^2].$$

For simplicity, we will often consider the setting where  $\rho$  has a density  $p$  expressed through a Gibbs potential  $V$ , which gradient would be the opposite of the “score”  $\nabla \log p$  in the generative AI vocabulary (Hyvärinen, 2005). Formally,  $\rho \ll dx$  with  $dx$  the Lebesgue measure, and for  $x \in \mathcal{X}$ ,

$$p(x) = \frac{\rho(dx)}{dx} = \frac{d\rho}{dx}(x) = \frac{1}{Z} \exp(-V(x)), \quad V(x) = -\log p(x) + C, \quad (4)$$

where  $Z$  is a normalization constant known as the partition function, and  $C = -\log(Z)$ . Under mild assumptions on  $p$ ,  $\mathcal{L}^{-1}$  is compact and  $\mathcal{L}$  is characterized as, see Appendix A.1,

$$\mathcal{L}f = -\Delta f + \langle \nabla V, \nabla f \rangle. \quad (5)$$

**Self-supervised learning.** The operator in (3) was the operator of choice for machine learning in the pre-deep learning area. Interestingly, many self-supervised learning algorithms can be seen as using variations of this operator. For example, the VICReg algorithm of Bardes et al. (2022) is built from on data augmentation  $\xi, \xi'$  generated conditionally to  $X$  and is stylized (when disregarding deep learning engineering tricks) as estimating spectral embeddings based on the operator  $\mathcal{L}_{\text{aug}}$  such that

$$\langle f, \mathcal{L}_{\text{aug}}g \rangle = \mathbb{E}_{X \sim \rho} [\mathbb{E}_{\xi, \xi'} [\langle f(\xi) - f(\xi'), g(\xi) - g(\xi') \rangle | X]], \quad (6)$$

where  $\xi$  and  $\xi'$  are two independent identically distributed random transformations of the input  $X$ . In essence, this corresponds to the introduction of a new geometry for the  $\nabla$  operator, which could be represented as a signed measure on  $\mathcal{X}^2$ ,

$$\nabla_{\text{aug}} f(x) = \mathbb{E}_{\xi, \xi'} [(f(\xi) - f(\xi'))\delta_{\xi, \xi'} | X = x] \in \text{Span } \Delta_{\mathcal{X}^2}.$$

Once again,  $\mathcal{L}_{\text{aug}}$  is a self-adjoint operator, indeed  $\mathcal{L}_{\text{aug}} = \nabla_{\text{aug}}^* \nabla_{\text{aug}}$  is a Laplacian. As mentioned earlier, spectral embeddings could also be defined through the singular value decomposition of an operator that is not necessarily self-adjoint or diagonalizable in  $L^2(\rho)$ . This is notably useful to model the large limits of the CLIP model (see the work of Lee et al., 2021, for a characterization of spectral embeddings behind CLIP).

## 2.2 Usefulness of spectral embeddings

The usefulness of the Laplacians, and more generally of spectral embeddings, for representation learning has been a long subject of discussion. In essence, Laplacian regularization, i.e. adding a regularization term  $\mathcal{E}_{\mathcal{L}}(f)$  on an objective to learn a function  $f$ , enforces the variations of  $f$  to be localized on low-density regions of the input space. The prior is that when inputs are close to one another they should have similar outputs, while if data are separated by region with no data, they

<sup>1</sup>Usually, Laplacians are defined as negative self-adjoint operators  $-\nabla^* \nabla$  as for the usual Laplacian  $\Delta = \sum \partial_{ii}^2$  which corresponds to adjunction with respect to  $L^2(dx)$  endowed with the Lebesgue measure. This paper rather uses the convention that Laplacian are positive self-adjoint operators.

could have different outputs. We refer the reader to the vast literature on the subject (Bousquet et al., 2003; Cabannes et al., 2023a). In terms of applications, it seems that the refined embedding defined by Coifman and Lafon (2006) has had the greatest impact. Their method, known as diffusion maps, impacted many different fields, such as molecular simulation (Glielmo et al., 2021), acoustics (Bianco et al., 2019) or the study of gene interaction (van Dijk et al., 2018) to name a few. More recently, the VICReg algorithm of Bardes et al. (2022) was shown to be an highly efficient way to get embeddings on raw images data consisting of arrays of pixels with neural network architectures.

**Some useful remarks for sampling.** While there exist many perspectives and algorithms to perform sampling, recent advances have showcased the usefulness of diffusion models in the realm of machine learning (see e.g. Dockhorn et al., 2022). One of the simplest diffusion model is the overdamped Langevin dynamics

$$dX_t = -\nabla V(X_t) dt + \sqrt{2\beta} dB_t. \quad (7)$$

In this equation, a random particle  $X$  is initialized at  $X_0$  and follows the evolution that  $X_{t+dt}$  equals  $X_t$  plus some random noise added by a Brownian motion model  $dB_t$  and a temperature parameter  $\beta$ , together with a drift  $\nabla V(X_t) dt$  which derives from a potential  $V$  and attracts  $X_t$  towards small values of  $V$ . Appendix A.2 details the evolution of the law of the particle. In essence for  $\beta = 1$ , if  $\mu_t$  is the law of  $X_t$ , the particle at time  $t$ , and if  $\nu = \mu_0$  has a density against  $\rho$ ,  $\mu_t$  follows the Fokker-Planck evolution

$$d\frac{d\mu_t}{d\rho} = -\mathcal{L}\frac{d\mu_t}{d\rho} dt, \quad (8)$$

where  $\mathcal{L}$  is defined as per (5), and  $\rho$  is the Gibbs density associated with the potential  $V$ . This leads to the following characterization of the Langevin dynamics, which can be seen as the dual of Monte-Carlo Markov chains and diffusion models, where rather than working on particles one works on densities.

**Proposition 1.** *The Langevin dynamics identifies as  $X_t \sim (\psi_t)_\# \nu$ , where  $\nu$  is the law of  $X_0$  (assumed to have a density) and  $\psi_t : \mathcal{X} \rightarrow \mathcal{X}$  is initialized at the identity  $\psi_0 = \text{id}$  and follows the gradient flow of the variational objective*

$$\psi \in \arg \min_{\psi: \mathcal{X} \rightarrow \mathcal{X}} \sum_{i \in \mathbb{N}} \lambda_i \mathbb{E}_{Z \sim \nu} [f_i(\psi(Z_1))]^2, \quad (9)$$

where  $(\lambda_i, f_i)$  is the spectral decomposition of  $\mathcal{L}$  in (3),  $\psi : \mathbb{R}^p \rightarrow \mathcal{X}$  is a pushforward maps to be learned (recall that  $X \sim \psi_\# \nu$  means  $X = \psi(Z)$  for  $Z \sim \nu$ ) and the differentiation is understood with respect to  $d\psi_\# \nu / d\rho$  in  $L^2(\rho)$ . Moreover, the solution of (9) verifies  $\rho = \psi_\# \nu$  for any  $\psi$  in the set of arguments of the minima, where  $\rho = \exp(-V) dx$  is the Gibbs density associated with  $V$ .

In simple terms, Proposition 1 states that  $X_t$  will converge in law towards  $X \sim \rho$ . Moreover, it implicitly shows how the mixing time of the Langevin diffusion is governed by  $\lambda_1^{-1}$ , which is known as the Poincaré constant, and corresponds to the time  $t$  to divide by a factor at most  $e$  the energy of  $(\psi_t)_\# \nu$  on the span of the  $(f_i)_{i \geq 1}$ , the bottleneck being due to the energy on low-frequencies, i.e. the eigenfunctions associated with small eigenvalues. In practice, it might preferable to follow a different dynamic, which could be done e.g. by replacing  $\lambda_i$  by  $h(\lambda_i)$  in (9) for  $h$  a decreasing function, assuming that the inductive bias of the architecture that parameterized  $\psi$  will easily remove the energy on the high frequencies functions (i.e. the  $f_i$  for big  $i \in \mathbb{N}$ ). The well-known fact that  $\rho$  is the stationary measure of the Langevin dynamics can be seen as a consequence of a more generic characterization of distributions stated by Theorem 1. While we are not aware of any links between representation learning and sampling, this will provide a useful characterization of distributions in order to turn data representations into sampling procedures.

**Theorem 1** (Pushforward sampler learned by function matching in a contrastive fashion). *Let  $\rho$  be a distribution deriving from a Gibbs potential  $V$ , and let  $\varphi \in L^2(\rho)^\mathbb{N}$  be a representation of the data under the form  $\varphi = U(c_i f_i)_{i \in \mathbb{N}}$  for  $(f_i)$  an orthogonal basis of  $L^2(\rho)$ ,  $f_0 = 1$  the constant function,*

$(c_i \neq 0)$  a set of non-null weights and  $U$  an orthogonal matrix on  $\ell^2$ . Then  $\rho$  is characterized for any  $p \in \mathbb{N}^*$  and any nonatomic distribution  $\nu \in \Delta_{\mathbb{R}^p}$  in  $\mathbb{R}^p$  as

$$\rho = \psi_{\#}(\nu); \quad \psi \in \arg \min_{\psi: \mathbb{R}^p \rightarrow \mathcal{X}} \mathbb{E}_{Z_1, Z_2 \sim \nu} [\langle \varphi(\psi(Z_1)), \varphi(\psi(Z_2)) \rangle], \quad (10)$$

where the equation (10) holds for any  $\psi$  in the set of minimizers.

**A new family of sampling algorithms.** Theorem 1 unveils a simple procedure to generate new samples when accessing a spectral representation  $\varphi$  built from functions  $f_i$  coming from the spectral decomposition of an operator in  $L^2(\mu)$  as long as constant functions are in the null space of  $\mathcal{L}$  as for the examples provided precedently (in which case our sampling procedure assimilates to Stein’s method (Stein, 1986)). Based on a original random variable  $Z \sim \nu$  for  $\nu$  chosen by the practitioner (e.g. a Gaussian variable in  $\mathbb{R}$ ), one can solve for  $\psi$  according to equation (10). Then new samples are generated in one step as  $X = \psi(Z)$  for  $Z \sim \nu$ . Note that while the base distribution  $\nu$  could be any continuous distribution *a priori*, its choice will condition the hardness to learn the pushforward map  $\psi$ . In terms of analogy with existing methods, the objective (10) could be seen as the opposite of an auto-encoder, given an encoder  $\varphi$ , one wants to learn a decoding  $\psi$  so that  $(\varphi \circ \psi)_{\#} \nu$  maps to  $\varphi_{\#} \rho$ , which can also be seen as statistics matching (per analogy with moment matching). It could also be seen as some form of non-adversarial GAN, where  $\varphi$  is some critic, and  $\psi$  wants to make sure that the evaluation of the critic averages to zero.

---

**Algorithm 1:** Learning pushforward sampler by implicit function matchings

---

**Data:** Representation  $\varphi: \mathcal{X} \rightarrow \mathbb{R}^m$  (2), initial distribution  $\nu \in \Delta_{\mathcal{Z}}$  for any sample space  $\mathcal{Z}$ .

**Result:** Samples  $(x_i)$  from the plausible underlying distribution  $\rho$ .

Fit a model  $\psi_{\theta}: \mathcal{Z} \rightarrow \mathcal{X}$  by minimizing the objective  $\mathcal{E}_{Z_1, Z_2 \sim \nu} [\langle \varphi(\psi_{\theta}(Z_1)), \varphi(\psi_{\theta}(Z_2)) \rangle]$ ;

Generate samples  $(z_i)$  from  $\nu$  and set  $x_i = \psi_{\theta}(z_i)$ .

---

### 3 Principles to build spectral embeddings

This section gathers different ideas from existing literature that can be used to estimate the spectral decomposition of an operator, or at least build representations as in Theorem 1 for  $(f_i)$  the eigenfunctions of  $\mathcal{L}$  and  $(c_i)$  defined from the corresponding eigenvalues. It focuses on operators  $\mathcal{L}: L^2(\rho) \rightarrow L^2(\rho)$  defining quadratic forms as expectations over the data, i.e.

$$\mathcal{E}_{\mathcal{L}}(f, g) = \langle f, \mathcal{L}g \rangle = \mathbb{E}_X [F(f, g, X)]$$

for some evaluable base operation  $F: L^2(\rho) \times L^2(\rho) \times \mathcal{X} \rightarrow \mathbb{R}$  that is supposed to be linear in both  $f$  and  $g$ . This is notably the form of the VICReg operator (6) and the Laplacian of (3) where  $F$  is defined as  $F(f, g, X) = \langle \nabla f(X), \nabla g(X) \rangle$ . For the sake of exposition clarity, some technical details are relegated to Appendix B.

#### 3.1 Empirical variational objectives

Based on Courant-Fischer min-max principle, one could search for the first  $m$  left and right singular functions of  $\mathcal{L}$  by optimizing the quantity, for  $\varphi^{\text{left}}, \varphi^{\text{right}}: \mathcal{X} \rightarrow \mathbb{R}^m$  with coordinates  $\varphi_i$ ,

$$\arg \max_{\varphi^{\text{left}}} \min_{\varphi^{\text{right}}} \mathcal{E}_{\mathcal{L}, m}(\varphi^{\text{left}}, \varphi^{\text{right}}) := \sum_{i \in [m]} \mathcal{E}_{\mathcal{L}}(\varphi_i^{\text{left}}, \varphi_i^{\text{right}}) = \mathbb{E}_{X \sim \rho} [F(\varphi_i^{\text{left}}, \varphi_i^{\text{right}}, X)].$$

together with the constraint that both the  $(\varphi_i^{\text{left}})$  and  $(\varphi_i^{\text{right}})$  should be orthonormal families in  $L^2(\rho)$ . For simplicity, we will focus on the symmetric case where  $F(f, g, \cdot) = F(g, f, \cdot)$  and more particularly on the case where  $\mathcal{L}$  is the Laplacian of (3). When  $F$  is not symmetric, the principles would work similarly, yet one would have to replace “eigen” with “singular”, and search for both the

left and the right singular functions simultaneously. In the symmetric case, one could search for the eigenfunctions of  $\mathcal{L}$  with  $\varphi : \mathcal{X} \rightarrow \mathbb{R}^m$  by minimizing

$$\arg \min_{\varphi} \mathbb{E}_{\mathcal{L}, m}(\varphi) := \sum_{i \in [m]} \langle \varphi_i, \mathcal{L} \varphi_i \rangle_{L^2(\rho)} = \mathbb{E}_{X \sim \rho} [F(\varphi, \varphi, X)] = \mathbb{E}_{X \sim \rho} [\|D\varphi(X)\|^2], \quad (11)$$

with the constraint that the  $(\varphi_i)$  should be orthogonal to one another in  $L^2(\mu)$ , where  $D$  denotes the Jacobian, the norm being the Frobenius norm on matrices. In machine learning settings, one does not access the distribution  $\rho$  but  $n$  samples  $(x_i)_{i \in [n]}$  thought as  $n$  independent realizations of the random variable  $X \sim \rho$ , hence approximation rules have to be found to estimate the objective (11).

**The case of graph-Laplacian.** Graph-Laplacians are the classical way to estimate Laplacian-related objectives in machine learning (Zhu et al., 2003; Belkin and Niyogi, 2003). Although there exist many variants, those methods mainly consist in approximating the Laplacian operator  $\mathcal{L}$  with finite differences. For  $f : \mathcal{X} \rightarrow \mathbb{R}$

$$\mathbb{E}[\|\nabla \varphi(X)\|^2] \approx \sum_{i, j \in [n]} w_{ij} (\varphi(x_i) - \varphi(x_j))^2, \quad (12)$$

where the  $w_{ij}$  are a set of weights usually taken as  $(w_{ij}) = D^{-1/2} \tilde{W} D^{-1/2}$  where  $\tilde{W}$  follows a Gaussian law  $\tilde{w}_{ij} \propto \exp(-\alpha \|x_i - x_j\|^2)$  with  $\alpha$  a scale parameter, and  $D = \text{diag}(\tilde{w}_{ii})$  is the degree matrix (associated with the weighted graph build on the  $n$  points with weights  $\tilde{w}_{ij}$ ). The approximation of the Laplacian operator with finite differences could be justified when  $f$  is thought of as a non-parametric model. However, this method is known to suffer from the curse of dimensionality (Bengio et al., 2006; Hein et al., 2007; Singer, 2006).

**Generic sub-sampling.** When  $\varphi$  is actually parameterized as  $\varphi_\theta$ , one might simply replace the expectation by the empirical expectation, and approximate  $\mathcal{E}_{\mathcal{L}}$  through the sub-sampling scheme

$$\mathbb{E}[F(\varphi_\theta, \varphi_\theta, X)^2] \approx n^{-1} \sum_{i \in [n]} F(\varphi_\theta, \varphi_\theta, x_i) = n^{-1} \sum_{i \in [n]} \|D\varphi_\theta(x_i)\|^2, \quad (13)$$

where the Jacobian has to be understood with respect to the input variable  $x \in \mathcal{X}$ . By replacing the finite differences approximation in (12) by the empirical summation of (13), one can actually get stronger guarantees on the statistical convergence of the estimated eigenfunctions towards the real ones (cf. Pillaud-Vivien and Bach, 2023, for the Laplacian case).

**Low-rank approximation.** The  $m$  gradients  $\nabla(\varphi_\theta)_i$  of the Jacobian matrix in the objective (13) are functions from  $\mathcal{X}$  to the tangent spaces of  $\mathcal{X}$  which can be really big, and eventually inconvenient to encode on a computer without low-rank approximation techniques. Those low-rank approximation techniques could be projections of the Jacobian onto some directions, e.g. leveraging the formula that for  $u$  a uniformly random direction on the sphere  $\mathcal{S}^{d-1}$  and any  $x$  in  $\mathcal{X} = \mathbb{R}^d$ ,

$$\|D\varphi_\theta(x)\| = c^{-1} \mathbb{E}_{u \sim \mathcal{U}} [\langle D\varphi_\theta(x), u \rangle^2], \quad c = \mathbb{E}[u_1^2] \approx \text{vol}(\mathcal{S}^{d-2}).$$

or by selecting certain particular directions such as the ones defined by  $\xi' - \xi$  for  $\xi$  and  $\xi'$  two random augmentations from  $x$ , which would higher the constant  $c$  in the latter objective, and accelerate convergence of stochastic gradient descent (SGD) on this objective (recall how SGD speed is determined by the standard deviation of the gradients, which depends linearly on  $c^{-1}$  in this case, cf. Bubeck (2015)).

For linear parameterization of each coordinate of  $\varphi$  under the form  $\varphi_\theta = \langle \theta, \kappa(x) \rangle$  for some Hilbert space  $\mathcal{H}$  and a feature map  $\kappa : \mathcal{X} \rightarrow \mathcal{H}$ , one could consider the reparameterization of  $\theta$  with  $a \in \mathbb{R}^p$  through  $\theta = \sum_{i \in [p]} a_i \kappa(y_i)$  for some predefined representer  $(y_i) \in \mathcal{X}^p$  and a small  $p$ . In molecular dynamics, this is similar to the Galerkin method, while in machine learning it resembles

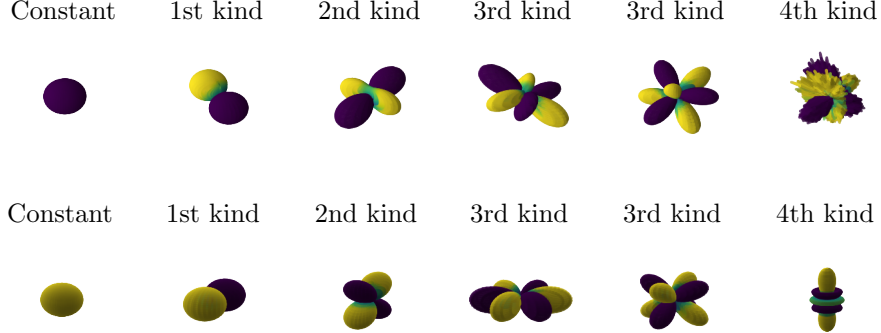


**Figure 1:** Learning spherical harmonics with polynomials of degree three (with  $k(x, y) = (1 + x^\top y)^3$  which corresponds to  $\kappa(x)$  concatenating all the multivariate monomials of degree smaller or equal to  $D = 3$ ). Like many diffusion operators, when  $\rho$  is uniform on the sphere, the operator  $\mathcal{L}$  is diagonalized by polynomials of increasing degrees (Bakry et al., 2021). The polynomial kernel of degree  $D$  allows to learn all the spherical harmonics of  $s$ -th kind for  $s$  smaller or equal to  $D$  (the ones of higher kind are polynomials of higher degree that can not be reconstructed with polynomials of degree  $D$  as illustrated with the fourth kind on the Figure). Some of the learned eigenfunctions are represented on the top row, while some ground truths are represented on the bottom row. Our method learned perfectly valid harmonics, although, for eigenvalues that are repeated, it does not learn the canonical ones, but any basis of the different eigenspaces (which can be observed with the harmonics of the second kind on the Figure).

Nyström subsampling. One could furthermore refer to the Rayleigh–Ritz method in numerical analysis. The approximation (13) becomes, with  $k(x, y) = \kappa(x)^\top \kappa(y)$ ,

$$\langle \varphi_\theta, \mathcal{L}\varphi_\theta \rangle \approx a^\top La, \quad L = (n^{-1} \sum_{l \in [n]} F(k(\cdot, y_i), k(\cdot, y_j), x_l))_{ij} \in \mathbb{R}^{p \times p}. \quad (14)$$

This will lead to a small eigenvalue problem in  $\mathbb{R}^p$ , although building  $L$  might require  $O(np^2c)$  where  $c$  is the cost of computing the  $F(k(\cdot, y_i), k(\cdot, y_j), x_k)$ . This cost is typically  $c = d$  in the Laplacian case (Cabannes et al., 2021), which could be quite prohibitive for large-scale applications. A main algorithmic contribution of this paper is to reduce it to  $c = 1$  for dot-product and translation-invariant kernels as detailed by Algorithms 2, 4 and proven in Appendix C. This seemingly innocuous improvement allows to match the sample complexity of Nyström kernel ridge regression, meaning that practitioners can now use Laplacian regularization while simply multiply by a small constant factor the total number of floating point operations of their methods (Meanti et al., 2020).

### 3.2 Orthogonality constraints

As mentioned earlier, the minimization of the variational objective (11) demands enforcing orthogonality constraints on the recovered eigenfunctions. Many methods could be proposed, such as naive iterative methods based on Courant-Fischer min-max principle; or using unitary-invariant objectives together with Cholesky decomposition at each gradient update with bilevel optimization (Pfau et al., 2019). This section proposes two efficient methods, an advanced one for kernel methods; and a simple one for neural network architecture.

**Generalized eigenvalues decomposition.** Classically, eigenfunctions are searched as parametric function  $\varphi_\theta : x \mapsto \theta^\top \kappa(x)$  through a mapping  $\kappa : \mathcal{X} \rightarrow \mathcal{H}$  for  $\mathcal{H}$  a separable Hilbert space, and a parameter  $\theta \in \mathcal{H}$  (Ham et al., 2004). Those “linear” models parameterize rich spaces of functions known as reproducing kernel Hilbert spaces. The full geometry of those spaces being captured by the kernel  $k(x, y) = \kappa(x)^\top \kappa(y)$ , those functions can actually be described through the sole use of a (reproducing) kernel  $k : \mathcal{X} \times \mathcal{X} \rightarrow \mathbb{R}$  (Scholkopf and Smola, 2001). Many  $k$ , such as the Gaussian kernel  $k(x, y) = \exp(-\|x - y\|^2)$  on  $\mathcal{X} = \mathbb{R}^d$ , are known to possess universal approximation properties, i.e. to enable the learning of any function (Micchelli et al., 2006).

It is useful to think with the mapping  $S : \mathcal{H} \rightarrow L^2(\rho); \theta \mapsto \varphi_\theta$  (Caponnetto and De Vito, 2006). In particular, the search for the spectral decomposition solving the system  $\mathcal{L}\varphi = \lambda\varphi$  can be solved through  $\mathcal{H}$  as  $\mathcal{L}S\theta = \lambda S\theta$ . Moreover, projecting this later system into  $\mathcal{H}$  leads to  $S^*\mathcal{L}S\theta = \lambda S^*S\theta$ . Two central operators on  $\mathcal{H}$  appears there, which, as explained in Appendix B, are simply defined as

$$\Sigma_{\mathcal{H}} = S^*S = \mathbb{E}_X[\kappa(X) \otimes \kappa(X)], \quad L_{\mathcal{H}} = S^*\mathcal{L}S = \mathbb{E}_X\left[\sum_{i=1}^d \partial_i \kappa(X) \otimes \partial_i \kappa(X)\right].^2 \quad (15)$$

The spectral decomposition of  $\mathcal{L}$  can be solved with the generalized spectral decomposition of  $(L_{\mathcal{H}}, \Sigma_{\mathcal{H}})$ . More in particular, under definition assumptions, if  $(\lambda_i, \theta_i)$  is the generalized eigendecomposition of  $(L_{\mathcal{H}}, \Sigma_{\mathcal{H}})$ , then  $(\lambda_i, \varphi_{\theta_i})$  is the eigendecomposition of  $\mathcal{L}$ . In particular, the orthogonal constraints on the  $(\varphi_{\theta_i})$  are enforced by the fact that

$$\langle \varphi_{\theta_i}, \varphi_{\theta_j} \rangle = (S\theta_i)^\top S\theta_j = \theta_i^\top \Sigma_{\mathcal{H}} \theta_j = \delta_{ij},$$

where the last equality is due to properties of the generalized eigendecomposition (Golub and Loan, 2013). In practice, the eigenfunctions of  $\mathcal{L}$  might not belong to our parametric models, and one might need to regularized the system as  $(L_{\mathcal{H}} + \varepsilon I, \Sigma_{\mathcal{H}})$  or  $(L_{\mathcal{H}}, \Sigma_{\mathcal{H}} + \varepsilon I)$  for a small regularizer  $\varepsilon > 0$  to avoid getting solution  $\theta_i = +\infty$ .

For the Galerkin method described precedently (14), the orthogonal constraints are cast with  $\Sigma = n^{-1}K^\top K \in \mathbb{R}^{p \times p}$  where  $K = (k(x_i, y_j)) \in \mathbb{R}^{n \times p}$ , and the spectral decomposition of  $\mathcal{L}$  is approximated from the generalized eigenvalue decomposition (GEVD) of  $(L, \Sigma)$ . Interestingly, this property of the GEVD seems to have never been utilized for graph-Laplacians.

---

**Algorithm 2:** Fast Laplacian spectral embeddings algorithm for dot-product kernel

---

**Data:** Datapoints  $(x_i) \in \mathcal{X}^n$ , a dot-product kernel  $k(x, y) = q(x^\top y)$ ,  $q : \mathbb{R} \rightarrow \mathbb{R}$ .

**Result:** Estimate  $(\lambda_i, f_i)$  of the spectral decomposition of  $\mathcal{L}$ .

Compute  $X = (x_i^\top x_j) \in \mathbb{R}^{p \times n}$ ;

Compute  $\Sigma = q(X)q(X)^\top \in \mathbb{R}^{p \times p}$  where  $q(X)$  is understood elementwise;

Compute  $L = (q'(X)q'(X)^\top)$ ; Update  $L_{ij} \leftarrow X_{ij}L_{ij}$  for all  $i, j \in [p]$ ;

Solve the generalized eigenvalues problems  $(\lambda_i, (a_{ij})_{j \in [p]})_{i \in [p]} \leftarrow \text{GEVD}(L, \Sigma)$ ;

Set  $f_i(x) := \sum_{j \in [p]} a_{ij}k(x, x_i)$ .

---

**Plain orthogonality constraints.** In the era of deep learning, fancy linear algebra considerations such as generalized spectral decompositions can be replaced by simple losses. In particular, when minimizing (11) with  $\varphi : \mathcal{X} \rightarrow \mathbb{R}^m$ , orthogonality constraints could be enforced through the regularizer for  $\varphi : \mathcal{X} \rightarrow \mathbb{R}^m$  parameterizing  $m$  eigenfunctions,

$$\mathcal{R}(\varphi) = \|\mathbb{E}_{X \sim \rho}[\varphi(X)\varphi(X)^\top] - I\|^2. \quad (16)$$

This regularizer is to relate with the Variance-Covariance regularizer (VCReg) in the realm of self-supervised learning (Bardes et al., 2022). In terms of spectral decomposition retrieval, for any  $\beta > 0$ , Lemma 2 of Cabannes et al. (2023b) states that the consequent energy minimization satisfies

$$\arg \min_{\varphi: \mathcal{X} \rightarrow \mathbb{R}^m} 2\beta \sum_{i \in [m]} \langle \varphi_i, \mathcal{L}\varphi_i \rangle + \mathcal{R}(\varphi) = \left\{ U(\sqrt{(1 - \beta\lambda_i)_+} f_i)_{i \in [m]} \mid U \in \mathbb{R}^{m \times m}; UU^\top = I \right\}, \quad (17)$$

where  $(\lambda_i, f_i)$  is the eigenvalue decomposition of  $\mathcal{L}$ , with  $\lambda_i$  in increasing order. In essence, the parameter  $\beta$  acts as a threshold parameter on the eigenvalues of  $\mathcal{L}$ , forbidding the retrieval of eigenfunctions associated with an eigenvalue that is bigger than  $\beta^{-1}$ . While the spectral decomposition of  $\mathcal{L}$  is only retrieved up to a rotation matrix  $U$  and a function  $\lambda \mapsto \sqrt{(1 - \beta\lambda)_+}$ , the solution could be rectified with PCA on the embedding space  $U\varphi^*(\mathcal{X})$  endowed with the push-forward distribution  $(U\varphi^*)\#\mu$ . However, for both representation learning, and the pushforward sampler algorithm, there is no need to solve  $(\lambda_i, f_i)$  in the representation. Appendix Q details our implementations.

---

**Algorithm 3:** Variational Laplacian framework with VCReg

---

**Data:** Datapoints  $(x_i) \in \mathcal{X}^n$ , a network architecture  $f_\theta : \mathcal{X} \rightarrow \mathbb{R}^m$ .

**Result:** Spectral embedding  $f_\theta = \text{rotation}(\sqrt{(1 - \lambda_i)_+} f_i)$  associated with  $\mathcal{L}$ .

Fit  $\theta$  by minimizing  $n^{-1} \sum_{i \in [n]} \|\nabla f_\theta(x_i)\|^2 + \|n^{-1} \sum_{i \in [n]} f_\theta(x_i) f_\theta(x_i)^\top - I\|^2$ .

---

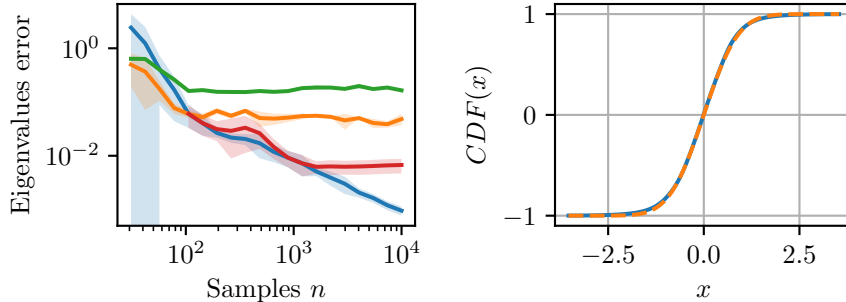


**Figure 2:** (Left) Testing error when learning the first 25 “spherical harmonics” eigenvalues with the exponential kernel (blue), the gaussian kernel (orange), graph-Laplacian (green), and the exponential kernel with 100 “Galerkin” representers (red). We notice the superiority of subsampling over graph-Laplacian (green vs all), the usefulness of taking a good kernel (orange vs blue), and the efficiency of Galerkin method (red vs blue). (Right) Learning the error function as the optimal mapping  $\psi$  to map the Gaussian distribution  $\mathcal{N}(0, 1)$  to the uniform distribution on  $[0, 1]$  with the objective (10) for  $\varphi$  defined by the first ten eigenfunctions of  $\mathcal{L}$  in (3), i.e.  $f_j(x) = \cos(2\pi(j - 1)x)$  with  $j \in [10]$  and  $c_j = 1$ . The ground truth, that relates to the error function, is plotted in dashed orange, while the learned CDF is plotted in blue. Experimental setups and reproducibility specifications are detailed in Appendix D.

## 4 Experiments

**Representation learning.** First of all, one can check that our techniques do learn eigenfunctions of the Laplacian operator  $\mathcal{L}$  (3) in settings where the ground truth is known. To this end, let us consider the sphere in  $\mathbb{R}^3$  with uniform distribution where the operator  $\mathcal{L}$  (3) identifies to the square of the orbital angular momentum (Condon and Shortley, 1935), whose eigenfunctions are known to be the spherical harmonics. Figure 1 illustrates how our Galerkin approach enables the learning of spherical harmonics. Moreover, the different methods could be compared by looking at the error made when estimating the corresponding eigenvalues, which is reported on Figure 2.

**Sampling.** Once again to check for soundness of our methods, one can consider settings where many quantities can be derived in closed-form. For example, when  $\mathcal{X}$  is one-dimensional and  $\nu$  is taken as the uniform distribution on  $[0, 1]$ , an optimal  $\psi$  in (10) is provided by the quantile function, in which case the consequent sampling procedure identifies with inverse transform sampling. Reciprocally, when  $\rho$  is taken as the uniform distribution on  $[0, 1]$ , then an optimal  $\psi$  is provided by the cumulative distribution function. As a proof of concept, Figure 2 illustrates how when choosing  $\nu = \mathcal{N}(0, 1)$  and  $\rho$  the uniform distribution on  $[0, 1]$ , one can learn the error function. In this latter setting,  $\mathcal{L}$  assimilates to  $-\Delta$  and its spectral decomposition is  $f_j = \cos(2\pi(j - 1)x)$ ,  $\lambda_j = 4\pi^2(j - 1)^2$ .

Additional experiments and details are provided in Appendix D.

## 5 Conclusion

This paper’s first aim was to convince the reader of the usefulness of spectral embeddings, notably the ones linked to the Laplacian operator  $\mathcal{L}$  in (3). With this perspective in mind, it introduces a new algorithm, the “pushforward sampler”, which has the advantage of providing fast sampling at inference time (sample  $Z \sim \nu$  and apply  $\psi$ ). This algorithm provides new avenues to link what is learned about the underlying structure of the data in generative AI and in representation learning. We

have then turned our attention to the estimation of those embeddings while only being given samples  $(X_i) \sim \rho^{\otimes n}$  rather than the full distribution  $\rho$ . We differentiate two techniques.

- Kernel-method techniques that offer strong statistical guarantees, extending recent algorithms (Pillaud-Vivien and Bach, 2023) and improving them as per Algorithms 2 and 4.
- Deep learning techniques that were proven successful in representation learning, extrapolating the underlying structure behind VICReg (Bardes et al., 2022) as per Algorithm 3.

**Limitations.** Although the losses to estimate spectral embeddings in this paper were designed to be convex on the cone of positive matrices  $\varphi(X)\varphi(X)^\top$ , when models are not convex, training dynamics might exhibit robustness and stability issues, and proper hyperparameters tuning might be required to induce behaviors of interest in neural networks. Those considerations related to deep learning engineering were not considered in this paper. Moreover, this paper heavily relies on linear structures in abstract spaces (operator on Hilbert spaces). While those structures are both powerful and easy to work with, it is not clear if they really capture what makes things work in practice. Finally, empirical validations on large datasets with high-dimensional inputs are missing, and it is not clear yet if the “pushforward sampler” could make a name for itself in the generative AI landscape. Indeed, it might find applications elsewhere, for example to define better initial distributions for the Metropolis-adjusted Langevin algorithm. In the meanwhile, spectral embeddings could yield good reaction coordinates (Wang et al., 2019), which could be used to modify Langevin dynamics to lower its mixing time (Comer et al., 2014; Dalalyan and Riou-Durand, 2018).

**Future work.** The introduction of the pushforward sampler raises many questions, both theoretical and empirical. In practice, we expect useful to stack several features into  $\varphi$ , e.g. on images, some features could have been learned with self-supervised learning, while others could be engineered to enforce super-resolution. In theory, we would like to deepen the duality where rather than transporting particles one learns a transport map directly. In particular, while gradient flow with a specific objective can be seen as following Langevin dynamics on measures, one may unveil links between other transports and gradient flow over objectives that might evolve over time, e.g.  $\mathcal{L} = \mathcal{L}_t$  could be the Laplacian linked to some mixed distribution  $t\rho + (1-t)\mathcal{N}(0, I)$  as in diffusion models (Song et al., 2021). More in general, the pushforward sampler presented in this paper might be one of many pushforward learning algorithms by function matching, and in practice it might be more interesting to learn  $\psi$  by matching characteristic functions with

$$\mathbb{E}_{Z_1, Z_2 \sim \nu} \left[ \int_{\mathbb{R}} (e^{it\psi(Z_1)} - \mathbb{E}_{X \sim \rho}[e^{itX}]) (e^{it\psi(Z_2)} - \mathbb{E}_{X \sim \rho}[e^{itX}]) \mu(dt) \right],$$

for some measure  $\mu$  on  $\mathbb{R}$ , which might lead to better conditioned gradients when performing backpropagation since the characteristic function only takes values that are bounded by one in modulus. Indeed, as explained in Appendix D, the objective used for Figure 2 can be seen as minimizing the real-part of this objective for  $\mu$  the counting measure on  $[10]/2$ .

**Reproducibility.** The code to reproduce the experiments is available on the author GitHub at <https://github.com/VivienCabannes/>, the kernel laplacian repository is also available on PyPI as the “klap” package (`$ pip install klap`).

**Acknowledgement.** The author would like to thanks Loucas Pillaud-Vivien, Alberto Bietti, Carles Domingo-Enrich, Aram-Alexandre Pooladian, Valentin de Bortoli, Ricky Chen, Yann Lecun and Leon Bottou for useful inputs.

## References

Christophe Andrieu, Nando de Freitas, Arnaud Doucet, and Michael Jordan. An introduction to MCMC for machine learning. *Machine Learning*, 2003.

Dominique Bakry, Ivan Gentil, and Michel Ledoux. *Analysis and Geometry of Markov Diffusion Operators*. Springer, 2014.

Dominique Bakry, Stepan Orevkov, and Marguerite Zani. Orthogonal polynomials and diffusion operators. *Annales de la Faculté des sciences de Toulouse*, 2021.

Randall Balestrier and Yann LeCun. Contrastive and non-contrastive self-supervised learning recover global and local spectral embedding methods. In *Advances in Neural Information Processing Systems*, 2022.

Adrien Bardes, Jean Ponce, and Yann LeCun. Vicreg: Variance-invariance-covariance regularization for self-supervised learning. In *International Conference on Learning Representations*, 2022.

Mikhail Belkin and Partha Niyogi. Laplacian eigenmaps for dimensionality reduction and data representation. *Neural Computation*, 2003.

Yoshua Bengio, Olivier Delalleau, and Nicolas Le Roux. Label propagation and quadratic criterion. In *Semi-Supervised Learning*. MIT Press, 2006.

Michael Bianco, Peter Gerstoft, James Traer, Emma Ozanich, Marie Roch, Sharon Gannot, and Charles-Alban Deledalle. Machine learning in acoustics: Theory and applications featured. *The Journal of the Acoustical Society of America*, 2019.

Olivier Bousquet, Olivier Chapelle, and Matthias Hein. Measure based regularization. In *Advances in Neural Information Processing Systems*, 2003.

Sébastien Bubeck. Convex optimization: Algorithms and complexity. *Foundations and Trends in Machine Learning*, 2015.

Vivien Cabannes, Loucas Pillaud-Vivien, Francis Bach, and Alessandro Rudi. Overcoming the curse of dimensionality with Laplacian regularization in semi-supervised learning. In *Advances in Neural Information Processing Systems*, 2021.

Vivien Cabannes, Alberto Bietti, and Randall Balestrier. On minimal variations for unsupervised representation learning. *ICASSP*, 2023a.

Vivien Cabannes, Bobak Kiani, Randall Balestrier, Yann LeCun, and Alberto Bietti. The SSL interplay: Augmentations, inductive bias, and generalization. *arXiv preprint arXiv:2302.02774*, 2023b.

Andrea Caponnetto and Ernesto De Vito. Optimal rates for the regularized least-squares algorithm. *Foundations of Computational Mathematics*, 2006.

Ting Chen, Simon Kornblith, Mohammad Norouzi, and Geoffrey Hinton. A simple framework for contrastive learning of visual representations. In *International Conference on Machine Learning*, 2020.

Sinho Chewi. *Log-concave sampling*. Draft, 2023.

Fan Chung. *Spectral Graph Theory*. American Mathematical Society, 1997.

Ronald Coifman and Stéphane Lafon. Diffusion maps. *Applied and Computational Harmonic Analysis*, 2006.

Jeffrey Comer, James Gumbart, Jérôme Hénin, Tony Lelièvre, Andrew Pohorille, and Christophe Chipot. The adaptive biasing force method: Everything you always wanted to know but were afraid to ask. *The Journal of the Physical Chemistry B*, 2014.

Edward Condon and George Shortley. *The Theory of Atomic Spectra*. Cambridge University Press, 1935.

Arnak Dalalyan and Lionel Riou-Durand. On sampling from a log-concave density using kinetic Langevin diffusions. *ArXiv*, 2018.

Tim Dockhorn, Arash Vahdat, and Karsten Kreis. Score-based generative modeling with critically-damped Langevin diffusion. In *International Conference on Learning Representations*, 2022.

Aldo Glielmo, Brooke Husic, Alex Rodriguez, Cecilia Clementi, Frank Noé, and Alessandro Laio. Unsupervised learning methods for molecular simulation data. *Chemical Reviews*, 2021.

Gene Golub and Charles Van Loan. *Matrix computations (4th edition)*. Johns Hopkins University Press, 2013.

Michael Greenacre. *Theory and Applications of Correspondence Analysis*. Academic Press, 1984.

Ulf Grenander and Michael Miller. Representations of knowledge in complex systems. *Journal of the Royal Statistical Society. Series B (Methodological)*, 1994.

Jihun Ham, Daniel Lee, Sebastian Mika, and Bernhard Schölkopf. A kernel view of the dimensionality reduction of manifolds. In *International Conference of Machine Learning*, 2004.

Jiequn Han, Jianfeng Lu, and Mo Zhou. Solving high-dimensional eigenvalue problems using deep neural networks: A diffusion monte carlo like approach. *Journal of Computational Physics*, 2020.

Jeff HaoChen, Colin Wei, Adrien Gaidon, and Tengyu Ma. Provable guarantees for self-supervised deep learning with spectral contrastive loss. In *Advances in Neural Information Processing Systems*, 2021.

Matthias Hein, Jean-Yves Audibert, and Ulrike von Luxburg. Graph Laplacians and their convergence on random neighborhood graphs. *Journal of Machine Learning Research*, 2007.

Jonathan Ho, Ajay Jain, and Pieter Abbeel. Denoising diffusion probabilistic models. In *Advances in Neural Information Processing Systems*, 2022.

Aapo Hyvärinen. Estimation of non-normalized statistical models by score matching. *Journal of Machine Learning Research*, 2005.

Richard Jordan, David Kinderlehrer, and Felix Otto. The variational formulation of the fokker-planck equation. *Journal of Mathematical Analysis*, 1998.

Jason Lee, Qi Lei, Nikunj Saunshi, and Jiacheng Zhuo. Predicting what you already know helps: Provable self-supervised learning. In *Advances in Neural Information Processing Systems*, 2021.

Qiang Liu and Dilin Wang. Stein variational gradient descent: A general purpose Bayesian inference algorithm. In *Advances in Neural Information Processing Systems*, 2016.

Giacomo Meanti, Luigi Carratino, Lorenzo Rosasco, and Alessandro Rudi. Kernel methods through the roof: handling billions of points efficiently. In *Advances in Neural Information Processing Systems*, 2020.

Charles Micchelli, Yuesheng Xu, and Haizhang Zhang. Universal kernels. *Journal of Machine Learning Research*, 2006.

David Pfau, Stig Petersen, Ashish Agarwal, David Barrett, and Kimberly Stachenfeld. Spectral inference networks: Unifying deep and spectral learning. In *International Conference on Learning Representations*, 2019.

Loucas Pillaud-Vivien and Francis Bach. Kernelized diffusion maps. *ArXiv*, 2023.

Gareth Roberts and Richard Tweedie. Exponential convergence of Langevin distributions and their discrete approximations. *Bernoulli*, 1996.

Robin Rombach, Andreas Blattmann, Dominik Lorenz, Patrick Esser, and Björn Ommer. High-resolution image synthesis with latent diffusion models. In *International Conference on Computer Vision and Pattern Recognition*, 2022.

Simo Särkkä and Arno Solin. *Applied Stochastic Differential Equations*. Cambridge University Press, 2019.

Bernhard Scholkopf and Alexander Smola. *Learning with kernels: support vector machines, regularization, optimization, and beyond*. MIT press, 2001.

Patrice Simard, Bernard Victorri, Yann LeCun, and John Denker. Tangent prop - a formalism for specifying selected invariances in an adaptive network. In *Advances in Neural Information Processing Systems*, 1991.

Amit Singer. From graph to manifold laplacian: The convergence rate. *Applied and Computational Harmonic Analysis*, 2006.

Yang Song, Jascha Sohl-Dickstein, Diederik Kingma, Abhishek Kumar, Stefano Ermon, and Ben Poole. Score-based generative modeling through stochastic differential equations. In *International Conference on Learning Representations*, 2021.

Charles Stein. Approximate computation of expectations. *Institute of Mathematical Statistics Lecture Notes, Monograph Series*, 1986.

David van Dijk, Roshan Sharma, Juozas Nainys, Kristina Yim, Pooja Kathail, Ambrose Carr, Cassandra Burdziak, Kevin R. Moon, Christine Chaffer, Diwakar Pattabiraman, Brian Bierie, Linas Mazutis, Guy Wolf, Smita Krishnaswamy, and Dana Pe'er. Recovering gene interactions from single-cell data using data diffusion. *Cell*, 2018.

Charles van Loan. Journal on numerical analysis. *Nature Communications*, 1976.

Yihang Wang, Joao Marcelo Lamim Ribeiro, and Pratyush Tiwary. Past–future information bottleneck for sampling molecular reaction coordinate simultaneously with thermodynamics and kinetics. *Nature Communications*, 2019.

Christopher Williams and Matthias Seeger. Using the Nyström method to speed up kernel machines. In *Advances in Neural Information Processing Systems*, 2000.

Jure Zbontar, Li Jing, Ishan Misra, Yann LeCun, and Stéphane Deny. Barlow twins: Self-supervised learning via redundancy reduction. In *International Conference of Machine Learning*, 2021.

Wei Zhang, Tiejun Li, and Christof Schütte. Solving eigenvalue pdes of metastable diffusion processes using artificial neural networks. *Journal of Computational Physics*, 2022.

Xiaojin Zhu, Zoubin Ghahramani, and John Lafferty. Semi-supervised learning using Gaussian fields and harmonic functions. In *International Conference of Machine Learning*, 2003.

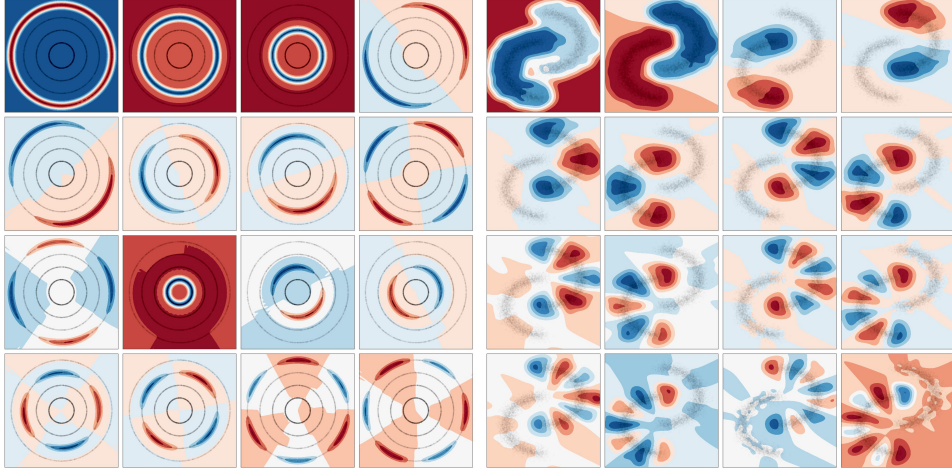


**Figure 3:** (Left) Level lines of the first sixteenth learned eigenfunctions of  $\mathcal{L}$  when the data generates concentric circles in 2d. Remark that the methods do not order the eigenfunctions correctly, which is due to estimation error when using  $n = 10^5$  points and  $p = 200$  with the Galerkin method and exponential kernel. (Right) Level lines of the learned eigenfunctions of  $\mathcal{L}$  when the data generates two half-moons in 2d. See how those eigenfunctions are separated between the two clusters, and how, on each cluster, they identify with Fourier modes (i.e. cosines) when distorting the segment  $[0, 1]$  into a half-moon.

## A Generic proofs

### A.1 Characterization of $\mathcal{L}$

The characterization of  $\mathcal{L}$  follows from multidimensional integration by part,

$$\begin{aligned}
\langle f, \mathcal{L}g \rangle_{L^2(\rho)} &= \int f(X)(\mathcal{L}g)(x)p(x) dx = \mathbb{E}[\langle \nabla f(X), \nabla g(X) \rangle] \\
&= \lim_{r \rightarrow +\infty} \sum_{i \in [d]} \int_{\|x\| < r} \underbrace{\partial_i f(x)}_{u'} \underbrace{p(x) \partial_i g(x)}_v dx \\
&= \lim_{r \rightarrow +\infty} \sum_{i \in [d]} \int_{\|x\| = r} \underbrace{f(x) p(x)}_u \underbrace{\partial_i g(x)}_v \langle e_i, n \rangle dS - \int_{\|x\| < r} \underbrace{f(x)}_u \underbrace{\partial_i(p(x) \partial_i g(x))}_{v'} dx \\
&= - \int f(x) \frac{1}{p(x)} \sum_{i \in [d]} \partial_i(p(x) \partial_i g(x)) p(x) dx,
\end{aligned}$$

where we used the fact  $p$  is regular enough, i.e.  $V$  is coercive. so that the surface integral goes to zero when  $g$  and  $f$  are smooth enough. As a consequence,

$$\begin{aligned}
(\mathcal{L}f)(x) &= -\frac{1}{p(x)} \sum_{i \in [d]} \partial_i(p(x) \partial_i f(x)) = -\frac{1}{p(x)} \sum_{i \in [d]} p(x) \partial_{ii}^2 f(x) + \partial_i p(x) \partial_i f(x) \\
&= -\Delta f(x) - \frac{1}{p(x)} \langle \nabla p(x), \nabla f(x) \rangle = -\Delta f(x) - \langle \nabla \log p(x), \nabla f(x) \rangle \\
&= -\Delta f(x) + \langle \nabla V(x), \nabla f(x) \rangle.
\end{aligned}$$

The compactness of  $\mathcal{L}^{-1}$  can be proven from Rellich–Kondrachov embedding theorem, which hold under mild regularity assumptions on  $\rho$  (see Assumption 0 in Pillaud-Vivien and Bach, 2023). This is useful to apply the spectral theorem and consider the countable eigenvalue decomposition of  $\mathcal{L}$ .

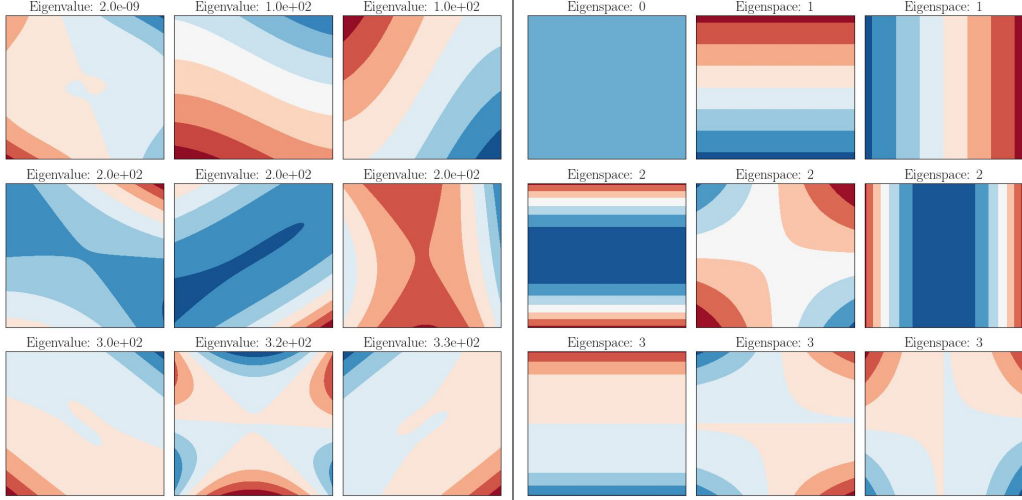


**Figure 4:** (Left) Level lines of the learned hermite polynomials in  $2d$  thanks to the operator  $\mathcal{L}$  with  $\mathcal{X} = \mathbb{R}^2$  and  $\rho = \mathcal{N}(0, I)$ , with polynomial kernel of degree 3. Compared to the ground truth on the right, notice how the learned polynomials are “random” basis of the different eigenspace of  $\mathcal{L}$  polynomials linear combination of the canonical polynomials (Right) Canonical Hermite polynomials, acting as a ground truth for the left part. The title indicates the eigenspace number that the eigenfunctions belong to. Any orthogonal transformation  $U(f_i)$  for  $(f_i)$  the  $k$  eigenfunctions of the  $k$ -th eigenspace, and  $U$  an orthogonal matrix in  $\mathbb{R}^{k \times k}$  is a valid basis of eigenfunctions of this eigenspace, which is what is found in practice.

## A.2 Primer on Langevin dynamics

This section recalls basic facts about Langevin dynamics.

**Evolution of test functions.** To study the stochastic differential equation in (7), one can consider its action on test functions  $h : \mathcal{X} \rightarrow \mathbb{R}$ . It follows from Itô calculus that the infinitesimal evolution of  $h(X_t)$  is governed by the equation.

$$\mathbb{E}_{dB_t}[dh(X_t)] = -\beta(\mathcal{L}_\beta h)(X_t) dt.$$

where  $\mathcal{L}_\beta$  is the Laplacian of (3) with density of potential  $\beta V$  in (4), e.g.  $\mathcal{L} = \mathcal{L}_1$ .

The last equation is proven with Itô formula (see e.g. Särkkä and Solin, 2019, Theorem 4.2), which states that the evolution of  $dh$  is governed by, writing  $X = X_t$  for simplicity,

$$dh(X) = \langle \nabla h(X), dX \rangle + \frac{1}{2} \text{Tr}((\nabla^2 h) dX dX^\top)$$

where  $\nabla^2$  is the Hessian of  $h$ , together with the rules that  $dB dt = dt dB = 0$ . As a consequence,

$$dh(X) = \left\langle \nabla h(X), -\nabla V(X) dt + \sqrt{2\beta} dB_t \right\rangle + \beta \text{Tr}(\nabla^2 h) dB dB^\top + o(dt)$$

Taking the expectation with respect to the Brownian motion, using that  $\mathbb{E}_{dB_t}[dB_t] = 0$  and  $\mathbb{E}_{dB_t}[dB_t dB_t^\top] = I dt$ ,

$$\begin{aligned} \mathbb{E}_{dB_t}[dh(X)] &= \langle \nabla h(X), -\nabla V(X) dt \rangle + \beta \text{Tr}(\nabla^2 h) dt + o(dt) \\ &= -\langle \nabla h(X), \nabla V(X) dt \rangle + \beta \Delta h dt + o(dt) \\ &= \beta (\Delta h - \langle \nabla h(X), \nabla(\beta V(X)) \rangle) dt + o(dt). \\ &= \beta \mathcal{L}_\beta h(X) dt + o(dt). \end{aligned}$$

This leads to a simple differential equation for  $\mathbb{E}_B h(X_t)$  which is solved with the operator exponential,  $e^A = \sum A^k/k!$ , for  $\mathbb{E}h(X_t) = \exp(-\beta t \mathcal{L}_\beta) X_0$ .

**Evolution of densities.** In the following, without loss of generality we will consider  $\beta = 1$ , the case  $\beta \neq 1$  corresponding to a rescaling of both the density and the time. Let  $\mu_t$  be the law of  $X_t$ . Rewriting the equation  $\mathbb{E}_B[h(X_t) | X_0] = (\exp(-t\mathcal{L})h)(X_0)$  with the duality bracket  $\langle h|\mu \rangle = \int h(x)\mu(dx)$ , it holds

$$\begin{aligned}\langle h|\mu_t \rangle &= \mathbb{E}_{X_0} \mathbb{E}_B[h(X_t) | X_0] = \mathbb{E}_{X_0}[(\exp(-t\mathcal{L})h)(X_0)] \\ &= \langle \exp(-t\mathcal{L})h|\mu_0 \rangle = \langle h|\exp(-t\mathcal{L}^*)\mu_0 \rangle,\end{aligned}$$

where the adjoint is taken with respect to the duality bracket. In other terms, the law of  $X_t$  follows the evolution

$$X_t \sim \mu_t = \exp(-t\mathcal{L}^*)\mu_0.$$

Under its infinitesimal form, this equation is written as

$$d\mu_t = -\mathcal{L}^* \mu_t dt.$$

When  $\mu$  has a density  $p$ , this adjoint corresponds to the adjoint with respect to the Lebesgue measure, and the density follows the evolution

$$dp_t = -t\mathcal{L}^* p_t dt, \quad p_t = \exp(-t\mathcal{L}^*)p_0.$$

The formula provided in the main text is the same formula expressed with density with respect to the measure  $\rho$  and with the adjoint in  $L^2(\rho)$  which is  $\mathcal{L}$  itself since  $\mathcal{L}$  is auto-adjoint in  $L^2(\rho)$ .

**Convergence of the dynamics.** Note that because of the Brownian motion  $X_{dt}$  will have a density against the Lebesgue measure, and since  $\rho \ll dx \ll \rho$  for any  $\rho$  that derives from a Gibbs potential, assuming that  $\nu = \mu_0$  has a density with respect to  $\rho$  is not a highly constraining assumption. In this setting, the evolution of the densities leads to, for  $(\lambda_i, f_i)$  the spectral decomposition of  $\mathcal{L}$  in  $L^2(\rho)$ ,

$$\frac{d\mu_t}{d\rho} = \exp(-t\mathcal{L}) \frac{d\nu}{d\rho} = \sum_{i \in \mathbb{N}} \exp(-t\lambda_i) \left\langle f_i, \frac{d\nu}{d\rho} \right\rangle_{L^2(\rho)} f_i = \sum_{i \in \mathbb{N}} \exp(-t\lambda_i) \langle f_i | \nu \rangle f_i.$$

As  $t$  goes to infinity, the density will converge with respect to the  $L^2(\rho)$ -topology towards

$$\frac{d\mu_\infty}{d\rho} = \sum_{i; \lambda_i=0} \langle f_i | \nu \rangle f_i = \langle f_0 | \nu \rangle f_0 = \langle 1 | \nu \rangle 1 = \nu(\mathcal{X})1 = 1.$$

In other terms,  $\mu_t$  will converge in law towards  $\rho$ .

**Gradient flow.** Let us now turn our attention to Proposition 1. We refer the reader to Jordan et al. (1998) for a more thorough presentation of links between Fokker-Planck equations and gradient flows on densities, which we have reparameterized in the proposition with a pushforward mapping. We have seen that the evolution of the law  $\mu_t$  of  $X_t$  was following an ordinary differential equation with base operator  $\mathcal{L}$ . Let us denote by  $p_t$  the density of  $\mu_t$  with respect to  $\rho$ , we reformulate its evolution as follows

$$\begin{aligned}dp_t = -\mathcal{L}p_t dt &= -\sum_{i \in \mathbb{N}} \lambda_i \langle f_i, p_t \rangle_{L^2(\rho)} f_i dt = -\sum_{i \in \mathbb{N}} \lambda_i \frac{d}{dp_t} \left( \langle f_i, p_t \rangle_{L^2(\rho)}^2 \right) dt \\ &= -\frac{d}{dp_t} \left( \sum_{i \in \mathbb{N}} \lambda_i \langle f_i, p_t \rangle_{L^2(\rho)}^2 \right) dt = -\frac{d}{dp_t} \left( \sum_{i \in \mathbb{N}} \lambda_i \langle f_i | \mu_t \rangle^2 \right) dt \\ &= -\frac{d}{dp_t} \left( \sum_{i \in \mathbb{N}} \lambda_i \mathbb{E}_{X \sim \mu_t} [f_i(X)]^2 \right) dt\end{aligned}$$

Let us parameterize  $X_t = \psi_t(X_0)$ . Note that this parameterization exists if and only if  $X_0$  is dominated by  $X_t$ , which is the case if  $X_0$  is dominated by  $\rho$ , or if  $X_0$  has a density.

$$d\frac{d(\psi_t)_{\#}\nu}{d\rho} = -\frac{d}{d\left(\frac{d(\psi_t)_{\#}\nu}{d\rho}\right)} \left( \sum_{i \in \mathbb{N}} \lambda_i \mathbb{E}_{Z \sim \nu} [f_i(\psi_t(Z))]^2 \right) dt.$$

**What about non Gibbs-density?** What happens for densities that follows the evolution  $p_t = \exp(-t\mathcal{L})p_0$  when  $\mathcal{L}$  is the Laplacian operator of (3) but  $\rho$  does not derive from a Gibbs potential. When  $\rho$  has  $k$  connected components  $(C_i)_{i \in [k]}$ , one could consider  $V+ = \infty$  outside the support of  $\rho$ . In this setting, the null space of  $\mathcal{L}$  is exactly the null space of  $\mathcal{E}_{\mathcal{L}}$ , which corresponds to the span of the indicator function  $\mathbf{1}_{C_i}$ . Therefore, all the density under the form  $\sum_{i \in I} \mathbf{1}_{C_i} a_i \exp(-V)$ , for any  $I \subset [k]$  and some weight  $(a_i) \in \mathbb{R}_+^I$ , would be stationary to the corresponding manifold constrained Langevin dynamics. As a consequence, the evolution of the measure of  $X_t$  satisfies a mass conservation property

$$\langle \mathbf{1}_{C_i} | dp_t \rangle = -\langle \mathbf{1}_{C_i} | \mathcal{L}^* p_t \rangle = -\langle \mathcal{L} \mathbf{1}_{C_i} | p_t \rangle = 0.$$

In other terms, the mass of  $\mu_t$  on each connected components  $C_i$  of  $\rho$  is conserved over time, leading to the weak convergence towards  $\sum_{i \in [k]} \langle \mathbf{1}_{C_i} | \mu_0 \rangle \rho|_{C_i}$  where  $\rho|_{C_i}$  is the law of  $(X | X \in C_i)$ . Hence, ensuring the convergence of Langevin dynamics towards the right distribution  $\rho$  requires careful tuning of the original distribution. Interestingly, in semi-, un-supervised, it is frequent to assume the cluster assumption, which implies that  $\rho$  has a disconnected support. This useful theoretical assumption for representation learning is rather cumbersome for sampling with Langevin dynamics or any pushforward sampler optimized with objective akin (10). Adding atomic mass to  $\rho$  would not change the picture.

### A.3 Characterization of $\rho$ through spectral embeddings

This subsection is devoted to the proof of Theorem 1. Let us consider a family  $(f_i)_{i \in \mathbb{N}}$  that generates  $L^2(\rho)$  with  $f_0 = 1$  and

$$\langle f_i, f_0 \rangle_{L^2(\rho)} = \langle f_i, 1 \rangle_{L^2(\rho)} = \mathbb{E}_{X \sim \rho}[f_i(X)] = 0,$$

as well as  $c \in \mathbb{R}^{\mathbb{N}}$  with  $c_i \neq 0$  and  $h : \mathbb{R} \rightarrow \mathbb{R}$  with  $h(x)$  achieving its minimum only in  $x = 0$ . We have the following characterization in the  $L^2(\rho)$  geometry

$$\mathbb{R} \cdot 1 = \otimes_{i \geq 1} f_i^\perp = \arg \min_{g: \mathcal{X} \rightarrow \mathbb{R}} \sum_{i \geq 1} c_i^2 h(\langle f_i, g \rangle_{L^2(\rho)}).$$

In terms of density with respect to the data measure, i.e.  $f = d\mu / d\rho$ , it translates into the characterization

$$\mathbb{R} \cdot \rho = \arg \min_{\mu \in \text{Span } \Delta_{\mathcal{X}}} \sum_{i \geq 1} c_i^2 h(\langle \varphi_i | \mu \rangle), \quad \langle h | \mu \rangle = \int h(x) \mu(dx).$$

Adding the constraints that those measure should be probability measure, when those space are one dimensional in  $L^2(dx)$  (which is the case when  $\rho$  dominates the Lebesgue measure as for Gibbs-densities), it holds

$$\rho = \arg \min_{\mu \in \Delta_{\mathcal{X}}} \sum_{i \in \mathbb{N}} c_i^2 h(\langle f_i | \mu \rangle), \quad (18)$$

where the addition of the first function  $f_0$  does not change the minimization since  $\langle f_0 | \mu \rangle = \langle 1 | \mu \rangle = \mu(\mathcal{X}) = 1$  is constant over the space of probability measures. In order to optimize over the space of measures we can parameterize them with pushforwards for any nonatomic measure  $\nu \in \mathbb{R}^p$  (or at least with a total atomic mass that is smaller than the one of  $\mu$ ) for any  $p \in \mathbb{N}^*$ ,

$$\begin{aligned} \rho &= \arg \min_{\psi_{\#} \nu; \psi: \mathcal{X} \rightarrow \mathbb{R}^p} \sum_{i \in \mathbb{N}} c_i^2 h(\langle f_i | \psi_{\#} \nu \rangle) = \arg \min_{\psi_{\#} \nu; \psi: \mathcal{X} \rightarrow \mathbb{R}^p} \sum_{i \in \mathbb{N}} c_i^2 h(\mathbb{E}_{X \sim \psi_{\#} \nu}[f_i(X)]) \\ &= \arg \min_{\psi_{\#} \nu; \psi: \mathcal{X} \rightarrow \mathbb{R}^p} \sum_{i \in \mathbb{N}} c_i^2 h(\mathbb{E}_{Z \sim \nu}[f_i(\psi(Z))]). \end{aligned}$$

**The quadratic case.** The main theorem corresponds to  $h(x) = x^2$ . In this setting, when  $U$  is an orthogonal matrix in  $\ell^2(\mathbb{N})$  so that  $U^\top U = I$ , using the fact that  $\mathbb{E}[A]^2 = \mathbb{E}[A_1]\mathbb{E}[A_2] = \mathbb{E}[A_1 A_2]$ ,

$$\begin{aligned} \sum_{i \in \mathbb{N}} c_i^2 h(\mathbb{E}_{Z \sim \nu}[f_i(\psi(Z))]) &= \sum_{i \in \mathbb{N}} c_i^2 \mathbb{E}_{Z \sim \nu}[f_i(\psi(Z))]^2 \\ &= \sum_{i \in \mathbb{N}} c_i^2 \mathbb{E}_{Z_1, Z_2 \sim \nu}[f_i(\psi(Z)) f_i(\psi(Z))] \\ &= \mathbb{E}_{Z_1, Z_2 \sim \nu}[\langle (c_i f_i(\psi(Z)))_{i \in \mathbb{N}}, (c_i f_i(\psi(Z)))_{i \in \mathbb{N}} \rangle] \\ &= \mathbb{E}_{Z_1, Z_2 \sim \nu}[\langle U(c_i f_i(\psi(Z)))_{i \in \mathbb{N}}, U(c_i f_i(\psi(Z)))_{i \in \mathbb{N}} \rangle] \\ &= \mathbb{E}_{Z_1, Z_2 \sim \nu}[\langle \varphi(\psi(Z)), \varphi(\psi(Z)) \rangle]. \end{aligned}$$

**Discussion on the weights.** Assuming that  $f_i$  are the eigenfunctions in (1), how to choose the weights  $(c_i)$  in the objective (10)? We argue in favor of taking  $c_i$  positive and being a decreasing function of the  $\lambda_i$  as in (2). If one looks at the law of  $X_t$  after following Langevin diffusion from a initial state  $X_0 \sim \nu$ , assuming  $\varphi_i = f_i$  (1),

$$\mu_t = \sum_{i \in \mathbb{N}} \exp(-\lambda_i t) \langle f_i | \nu \rangle f_i \nu.$$

Optimizing the initial distribution  $\nu$  in order to minimize the  $\chi^2$ -divergence between  $\mu_t$  and  $\rho$  under a set of constraint  $\mathcal{C}$  reads

$$\begin{aligned} \nu \in \arg \min_{\mu \in \mathcal{C}} & \left\| \sum_{i \in \mathbb{N}} \exp(-\lambda_i t) \langle f_i | \nu \rangle f_i - 1 \right\|_{L^2(\rho)}^2 \\ &= \arg \min_{\mu \in \mathcal{C}} \left\| \sum_{i \in \mathbb{N}^*} \exp(-\lambda_i t) \langle f_i | \nu \rangle f_i \right\|_{L^2(\rho)}^2 \\ &= \arg \min_{\mu \in \mathcal{C}} \sum_{i \in \mathbb{N}^*} \exp(-2\lambda_i t) \langle f_i | \nu \rangle^2. \end{aligned}$$

In other terms, when  $\varphi$  is chosen as the diffusion maps embedding, the objective (10) assimilates to the  $\chi^2$  divergence between the law of Langevin dynamic of  $X_{\beta t/2}$  when initialize at  $X_0 \sim \nu$  and  $\rho$ .

This paper does not resort to Langevin dynamics for sampling, yet we still argue that it makes sense to take  $(c_i)$  as a decreasing function of the  $\lambda_i$ . Indeed, for large  $i \in \mathbb{N}$ ,  $f_i$  corresponds to high-frequency harmonics, and we expect the inductive bias of the kernel or the deep network architecture and its optimization scheme to filter out such components in the learned density  $d\mu/d\rho$ . Instead the loss should focus on working on the low-frequency harmonics that encodes for rich information about our datasets.

**A remark for future work on optimal transport.** Note that when the sample variable  $Z$  lives in the same space as original samples  $X$ , if one wants to the map  $\psi$  to resemble optimal transport, one could add a penalization in the loss of (10) that measure the transport cost of  $\psi$ ,

$$\mathcal{R}_{\text{transport}}(\psi) = \mathbb{E}_{Z \sim \nu}[\|Z - \psi(Z)\|^2].$$

Having chosen the  $\nu$  to have less atomic mass than  $\rho$ , learning a deterministic transport map should not induce the usual problem tackled by Kontorovich relaxation of the Monge problem.

## B Primer on spectral embeddings

Most of those paper results are based on simple facts about abstract mathematical objects. Since those objects might not be familiar to the reader, the following section aimed at providing a self-contained picture on them. Let us consider two operators  $\mathcal{U}$  and  $\mathcal{V}$  from  $L^2(\rho)$  onto  $L^2(\rho, \mathcal{T})$  for some Hilbert

space  $\mathcal{T}$  such that  $\mathcal{L} = \mathcal{U}^* \mathcal{V}$ . In the main text, examples were given with  $\mathcal{U} = \mathcal{V} = \nabla$  (and  $\mathcal{T} = \mathbb{R}^d$ ). The quadratic form associated with  $\mathcal{L}$  reads

$$\langle f, \mathcal{L}g \rangle_{L^2(\rho)} = \langle \mathcal{U}f, \mathcal{V}g \rangle_{L^2(\rho)} = \mathbb{E}_{X \sim \rho} [\langle (\mathcal{U}f)(X), (\mathcal{V}g)(X) \rangle_{\mathcal{T}}].$$

This corresponds to

$$F(f, g, X) = \langle (\mathcal{U}f)(X), (\mathcal{V}g)(X) \rangle_{\mathcal{T}}.$$

While any operator can be written in this fashion, we will suppose that we can evaluate  $F$ , i.e.  $F$  only depends on known quantities. We will equally assume that the spectrum of  $\mathcal{L}^* \mathcal{L}$  is discrete, so that we do not have to deal with technicalities related to continuous spectra. Finally, we will focus on the singular functions associated with the smallest singular values. There are no difficulties to focus on the top ones instead.

**Proposition 2** (Courant-Fisher characterization). *The first singular spaces of dimension  $m$ ,  $E_m^{\text{left}} := \text{Span}\{f_i^{\text{left}}\}_{i \leq m}$  and  $E_m^{\text{right}} := \text{Span}\{g_i^{\text{right}}\}_{i \leq m}$  denoting by  $f_i^{\text{left}}$  and  $g_i^{\text{right}}$  the left and right singular values of  $\mathcal{L}$ , are characterized from the arguments of the optima*

$$((f_i^*), (g_i^*)) \in \arg \max_{(f_i) \text{ ortho.}} \min_{(g_i) \text{ ortho.}} \sum_{i < m} \langle f_i, \mathcal{L}g_i \rangle, \quad (19)$$

with

$$E_m^{\text{left}} = \text{Span} \{f_i^* \mid i \leq m\}, \quad E_m^{\text{right}} = \text{Span} \{g_i^* \mid i \leq m\}.$$

*Proof.* Recall that singular values  $\sigma_i(\mathcal{L})$  of an operator  $\mathcal{L}$  can be defined from the eigenvalues  $\lambda_i(\mathcal{L}^* \mathcal{L})$  of its square. The first one is defined as

$$\max_{f: \|f\|=1} \min_{g: \|g\|=1} \langle f, \mathcal{L}g \rangle_{L^2(\rho)} = \min_{g: \|g\|=1} \|\mathcal{L}g\|_{L^2(\rho)} = \min_{g: \|g\|=1} \langle g, \mathcal{L}^* \mathcal{L}g \rangle_{L^2(\rho)}^{1/2} = \lambda_0(\mathcal{L}^* \mathcal{L}).$$

Similarly, for any  $m \in \mathbb{N}$ , the first  $m$  singular values verify

$$\begin{aligned} \sum_{i < m} \sigma_i(\mathcal{L}) &= \max_{(f_i) \text{ ortho.}} \min_{(g_i) \text{ ortho.}} \sum_{i < m} \langle f_i, \mathcal{L}g_i \rangle \leq \max_{(f_i): \|f_i\|=1} \min_{(g_i) \text{ ortho.}} \sum_{i < m} \langle f_i, \mathcal{L}g_i \rangle \\ &= \min_{(g_i) \text{ ortho.}} \sum_{i < m} \|\mathcal{L}g_i\| = \sum_{i < m} \lambda_i(\mathcal{L}^* \mathcal{L}) \\ &= \sum_{i < m} \left\| \mathcal{L}g_i^{\text{(right)}} \right\| = \max_{(f_i) \text{ ortho.}} \min_{(g_i) \text{ ortho.}} \sum_{i < m} \langle f_i, \mathcal{L}g_i \rangle. \end{aligned}$$

Any arguments of the optima will generate the first  $m$  singular spaces.  $\square$

Note that Proposition 2 implies that for any argument  $((f_i^*), (g_i^*))$  of the optima of (19), there exists two rotation matrices  $R_1, R_2 \in \mathbb{R}^{m \times m}$ , with  $R^T R = I$ , such that

$$(f_i^*)_{i < m} = R(f_i^{\text{left}})_{i < m}, \quad (g_i^*)_{i < m} = R(g_i^{\text{right}})_{i < m}.$$

**An advantage of graph-Laplacian.** It should be noted that our methods rely on the fact that  $F$  is easy to evaluate, which is the case when  $F(f, g, x) = \langle \nabla f(x), \nabla g(x) \rangle$ . However, one could look at embeddings associated with operators that can not be represented with such a  $F$ , this is notably the case when looking for the diffusion operator on the manifold of the data endowed with uniform density, then  $F(f, g, x) = \langle \nabla_{\mathcal{M}} f, \nabla_{\mathcal{H}} g \rangle d_{\mathcal{M}} x / d\rho$  where  $d_{\mathcal{M}} x$  denotes the Lebesgue measure on the manifold  $\mathcal{M}$ , and the gradient is the Riemannian gradient. It turns out that proper reweighting of graph-Laplacians can approximate such an operator, while it is unclear how our methods would work to do so.

## B.1 Primer on kernel methods.

Let us focus on the search of singular functions with a parametric model  $f_\theta : \mathcal{X} \rightarrow \mathbb{R}; x \mapsto \langle \theta_i, \kappa(x) \rangle$  with  $\kappa : \mathcal{X} \rightarrow \mathcal{H}$  in  $L^2(\rho, \mathcal{H})$  with  $\mathcal{H}$  a separable Hilbert space and  $\theta \in \mathcal{H}$ . Note that  $\mathcal{H}$  can be reduced to the closure of the span of the  $\kappa(x)$ , which we will assume to be true in the following for simplicity.

**Central operators.** Let us define the embedding of  $\mathcal{H}$  in  $L^2(\rho)$  as

$$S : \mathcal{H} \rightarrow L^2(\rho); \theta \mapsto (x \mapsto \langle \theta, \kappa(x) \rangle).$$

Its adjoint verifies

$$S^* : L^2(\rho) \rightarrow \mathcal{H}; f \mapsto \mathbb{E}_{X \sim \rho}[f(X)\kappa(X)],$$

and its square

$$\Sigma_{\mathcal{H}} = S^*S : \mathcal{H} \rightarrow \mathcal{H}; \theta \mapsto \mathbb{E}_{X \sim \rho}[\kappa(X) \otimes \kappa(X)]\theta.$$

*Proof.* We can compute the adjoint of  $S^* : L^2(\rho) \rightarrow \mathcal{H}$  with  $\theta \in \mathcal{H}$  and  $f \in L^2(\rho)$  with

$$\langle S^*f, \theta \rangle_{\mathcal{H}} = \langle f, S\theta \rangle_{L^2(\rho)} = \mathbb{E}_{X \sim \rho}[f(X)\kappa(X)^\top \theta] = \mathbb{E}_{X \sim \rho}[f(X)\kappa(X)]^\top \theta.$$

Similarly for the square, the fact that

$$S^*S\theta = \mathbb{E}[(S\theta)(X)\kappa(X)] = \mathbb{E}[\langle \theta, \kappa(X) \rangle \kappa(X)] = \mathbb{E}[\kappa(X) \otimes \kappa(X)]\theta$$

ends the proof of the lemma.  $\square$

The singular value problem  $\sigma f = \mathcal{L}g$ , can be parameterized from  $\mathcal{H}$  with  $\sigma S\theta_1 = \mathcal{L}S\theta_2$  with  $\theta_1, \theta_2 \in \mathcal{H}$ . When  $\mathcal{H}$  is rich enough so that  $S(\mathcal{H})$  is dense in  $L^2(\rho)$ , which is true for usual kernels (Micchelli et al., 2006), the latter system written in  $L^2(\rho)$  can be cast in  $\mathcal{H}$  with  $S^*$  as  $S^*\mathcal{L}S\theta_2 = \sigma S^*S\theta_1$ .  $S^*\mathcal{L}S$  operates on  $\mathcal{H}$  linearly, and for  $x, x' \in \mathcal{X}$

$$\kappa(x)^\top S^*\mathcal{L}S\kappa(x') = \mathbb{E}_{X \sim \rho}[F(k(\cdot, x), k(\cdot, x'), X)],$$

where  $k : \mathcal{X} \times \mathcal{X} \rightarrow \mathbb{R}$  is defined as  $k(x, x') = \kappa(x)^\top \kappa(x')$ . Note that the action of any linear operator on  $\mathcal{H}$  is completely determined by its action on the  $\kappa(x)$ , since their span is dense in  $\mathcal{H}$ .

For the Laplacian example in the main text

$$S^*\mathcal{L}S = \mathbb{E}_{X \sim \rho} \left[ \sum_{i \in [d]} \partial_i \kappa(X) \otimes \partial_i \kappa(X) \right].$$

*Proof.* The proof follows from the definitions

$$\begin{aligned} F(S\theta_1, S\theta_2, x) &= \sum_{i \in [d]} \partial_i(S\theta_1)(x) \cdot \partial_i(S\theta_2)(x) = \sum_{i \in [d]} \partial_i \theta_1^\top \kappa(x) \cdot \partial_i \theta_2^\top \kappa(x) \\ &= \sum_{i \in [d]} \theta_1^\top \partial_i \kappa(x) \cdot \theta_2^\top \partial_i \kappa(x) = \theta_1^\top \sum_{i \in [d]} \partial_i \kappa(x) \cdot (\partial_i \kappa(x))^\top \theta_2 = \theta_1^\top \sum_{i \in [d]} (\partial_i \kappa(x) \otimes \partial_i \kappa(x)) \theta_2. \end{aligned}$$

Integrating over  $x$  leads to

$$\theta_1^\top S^*\mathcal{L}S\theta_2 = \langle S\theta_1, \mathcal{L}S\theta_2 \rangle = \theta_1^\top \mathbb{E}_{X \sim \rho} \left[ \sum_{i \in [d]} \partial_i \kappa(X) \otimes \partial_i \kappa(X) \right] \theta_2.$$

This explains the formula in the main text.  $\square$

More generally, one can create an algebraic structure to make sense of the equality

$$S^*\mathcal{L}S = \mathbb{E}_{X \sim \rho} [\mathcal{U}\kappa(X) \otimes \mathcal{V}\kappa(X)].$$

Abstractly, we can built  $\mathcal{U}\kappa(x) \otimes \mathcal{V}\kappa(x')$  as the quadratic form on  $\mathcal{H}$  that maps  $(\theta_1, \theta_2)$  to  $\langle (\mathcal{U}(S\theta_1))(x), (\mathcal{V}(S\theta_2))(x) \rangle_{\mathcal{Y}}$ . The tensor product can be understood to be the outer product on  $\mathcal{T}^{\mathcal{H}}$  with the  $\ell^2$ -product topology on top of the Hilbertian one on  $\mathcal{H}$ . The extension of  $\mathcal{U}$  to the mapping  $\kappa \in L^2(\rho, \mathcal{H})$  is understood coordinate-wise onto  $L^2(\rho, \mathcal{T}^{\mathcal{H}}) = L^2(\rho, \mathcal{T})^{\mathcal{H}}$ .

**Representer theorem.** So far, everything has been expressed either in  $L^2(\rho)$  or in  $\mathcal{H}$ , which does not lead to equations that can be explicitly implemented on silicon chips. When the expectations are replaced by empirical expectations over collected data  $(x_i)_{i \in [n]}$ , a trick is to realize that the solutions lie in the span of the different quantities that appear in the objectives. This fact, which is due to the Hilbertian nature of both our objectives and our models, is known as the representer theorem. In the Laplacian case, those different quantities are  $\kappa(x_j)$  and  $\partial_i \kappa(x_j)$  for  $j \in [n]$  and  $i \in [k]$ , meaning that any eigenfunction can be searched under the form

$$f(x) = \sum_{j \in [n]} a_j \kappa(x_j) + \sum_{i \in [d]} b_{ij} \partial_i \kappa(x_j),$$

for  $a \in \mathbb{R}^n$  and  $b \in \mathbb{R}^{nd}$ . However, rewriting the system  $L\theta = \lambda \Sigma_{\mathcal{H}}\theta$  with  $(a, b)$  will lead to an inconvenient linear system with  $n(d + 1)$ -variables, which would yield an algorithmic complexity in  $O(n^3 d^3)$ . One may wonder why when starting with  $\theta \in \mathcal{H}$ , we rewrote the system with  $\theta' \in \mathcal{H} \times \partial_1 \mathcal{H} \times \dots \times \partial_d \mathcal{H}$ , in the sense that parameterization of the form, for  $\mu$  a measure on  $\mathcal{X}$  that identifies to  $a$ ,

$$f : x \mapsto \int \langle \kappa(x), \kappa(y) \rangle_{\mathcal{H}} d\mu(y),$$

we ended up with parameterization in, with new measures  $(\mu_i)$  that identify to the  $b_i$ ,

$$f : x \mapsto \int \langle \kappa(y), \kappa(x) \rangle_{\mathcal{H}} d\mu(y) + \sum_i \int \langle \kappa(y), \partial_j \kappa(x) \rangle_{\mathcal{H}} d\mu_i(y).$$

This is where we need to drop out the representer theorem, and switch to another understanding on how to turn equations in  $\mathcal{H}$  or  $L^2(\rho)$  onto computer chips.

**Low-rank approximation.** Since  $\mathcal{H}$  is a separable Hilbert space, it admits an orthogonal basis  $(v_i)$  which can be used to cast equations from  $\mathcal{H}$  to  $\mathbb{R}^n$ , as well as any other family  $(u_i)$  that generates  $\mathcal{H}$ . Using the fact that  $\mathcal{H}$  can be reduced to the closure of the linear span of the  $\varphi(x)$ , such a basis can be built with Gram-Schmidt procedures with the sole access of  $k : \mathcal{X} \times \mathcal{X} \rightarrow \mathbb{R}$ . Based on data, we only need to describe the span of the quantities that appear in the empirical objective, that is the  $\kappa(x_i)$  and  $\partial_j \kappa(x_i)$ , in the Laplacian case. It turns out that this span can be relatively well approximated with  $u_i = \kappa(y_i)$  for  $i \in [p]$  with  $y_i$  that looks like the data (Williams and Seeger, 2000). It leads to the new parameterization

$$\theta = \sum_{i \in [p]} a_i \kappa(y_i),$$

with  $a \in \mathbb{R}^p$ . With this parameterization, we instantiate

$$\theta^\top S^* \mathcal{L} S \theta = a^\top L_\rho a, \quad L_\rho = \left( \langle k(\cdot, y_i), \mathcal{L} k(\cdot, y_j) \rangle_{L^2(\rho, \mathcal{T})} \right)_{ij} \in \mathbb{R}^{p \times p}. \quad (20)$$

Exhibiting more explicitly the expectation that is going to be replaced by the empirical one in practice, and illustrating it with the Laplacian example of the main text,

$$[L_\rho]_{ij} = \mathbb{E}_X [F(k(\cdot, y_i), k(\cdot, y_j), X))]_{ij} = \mathbb{E}_X [\langle \nabla_y k(X, y_i), \nabla_y k(X, y_j) \rangle_{\mathbb{R}^d}]. \quad (21)$$

Regarding the orthogonality constraints, the quadratic form  $\theta^\top S^* S \theta$  is rewritten as

$$\theta^* \Sigma_{\mathcal{H}} \theta = a^\top \Sigma_\rho a, \quad \Sigma_\rho = (\mathbb{E}_X [k(X, y_i) k(X, y_j)])_{ij} \in \mathbb{R}^{p \times p}. \quad (22)$$

Replacing the expectation over  $\rho$  by the expectation over the data leads to the  $(\Sigma, L)$  defined in the main text.

## B.2 Primer on generalized singular value decomposition

**GSVD definition.** First of all, let us warn the reader that there are two different notions of generalized singular value decomposition (GSVD). While the generic algorithm of Cabannes et al. (2021) made use of the two-matrices version of van Loan (1976), we will use the weighted single-matrix one that appeared in correspondence analysis (Greenacre, 1984). Based on three matrices

$$(L, \Sigma_1, \Sigma_2) \in \mathbb{R}^{p_1 \times p_2} \times \mathbb{R}^{p_1 \times 1} \times \mathbb{R}^{p_2 \times p_2},$$

it finds three matrices, with  $p = \min(p_1, p_2)$ ,

$$(A, B, S) \in \mathbb{R}^{p_1 \times p} \times \mathbb{R}^{p_2 \times p} \times \text{diag}(\mathbb{R}_+^p),$$

that satisfies

$$L = ASB^\top, \quad A^\top \Sigma_1 B = I_{p_1}, \quad A^\top \Sigma_2 B = I_{p_2}. \quad (23)$$

*Proof.* The existence of such a decomposition follows from considering the eigenvalues decomposition of  $\Sigma_1^{1/2} L \Sigma_2^{1/2} = USV^\top$  and setting  $A = \Sigma_1^{1/2} U$ ,  $B = \Sigma_2^{1/2} V$ .  $\square$

**Galerkin method.** Let us recall that we are trying to solve the system, for  $m \in \mathbb{N}$ ,

$$\max_{f \in \mathcal{C}_m} \min_{g \in \mathcal{C}_m} \sum_{i \in [m]} \langle f_i, \mathcal{L}g_i \rangle_{L^2(\rho)}, \quad (24)$$

where  $\mathcal{C}$  is the set of functions from  $\mathcal{X}$  to  $\mathbb{R}^m$  whose coordinates are orthogonal in  $L^2(\rho)$ . To solve this system, we can parameterize the coordinates  $(f_j)_{j \in [m]}, (g_j)_{j \in [m]}$  thanks to  $p_1, p_2$  functions  $\alpha_i, \beta_i$  in  $L^2(\rho_{\mathcal{X}})$  as

$$f_j = \sum_{i \in [p_1]} a_{ij} \alpha_i(x), \quad g_j = \sum_{i \in [p_2]} b_{ij} \beta_i(x), \quad (25)$$

with  $A = (a_{ij}) \in \mathbb{R}^{p_1 \times m}$  and  $B \in \mathbb{R}^{p_2 \times m}$ . To unify notations, let  $(C, \gamma, i) \in \{(A, \alpha, 1), (B, \beta, 2)\}$ . The parameterization (25) can be cast in the operator framework with

$$\mathcal{Z}_C : \mathbb{R}^{p_C} \rightarrow L^2(\rho); c \mapsto \sum_{j \in [p_i]} c_j \gamma_j.$$

Under this parameterization, the system (24) becomes

$$\max_{A \in \mathcal{C}_A} \min_{B \in \mathcal{C}_B} \text{Tr}(A^\top LB), \quad L = \mathcal{Z}_A^* \mathcal{L} \mathcal{Z}_B \in \mathbb{R}^{p_1 \times p_2}, \quad L_{ij} = \mathbb{E}_X[F(\alpha_i, \beta_j, X)], \quad (26)$$

where

$$\mathcal{C}_C = \{C \in \mathbb{R}^{m \times p_i} \mid C^\top \Sigma_C C = I\}, \quad \Sigma_C = Z_C^* Z_C, \quad [\Sigma_C]_{ij} = \mathbb{E}_X[\gamma_i(X) \gamma_j(X)]. \quad (27)$$

This system is solved for

$$(S, A, B) = \text{GSVD}(L, \Sigma_A, \Sigma_B). \quad (28)$$

When  $\rho$  is replaced by  $n^{-1} \sum_{i \in [n]} \delta_{x_i}$ , it can be implemented on computers.

*Proof.* The objective is rewritten as

$$\begin{aligned} \sum_{i \in [m]} \langle f_i, \mathcal{L}g_i \rangle_{L^2(\rho)} &= \sum_{i \in [m]} \langle \mathcal{Z}_A a_i, \mathcal{L} \mathcal{Z}_B b_i \rangle_{L^2(\rho)} = \sum_{i \in [m]} \langle a_i, \mathcal{Z}_A^* \mathcal{L} \mathcal{Z}_B b_i \rangle_{\mathbb{R}^{p_1}} \\ &= \sum_{i \in [m]} a_i^\top \mathcal{Z}_A^* \mathcal{L} \mathcal{Z}_B b_i = \text{Tr} \left( \mathcal{Z}_A^* \mathcal{L} \mathcal{Z}_B \sum_{i \in [m]} b_i a_i^\top \right) = \text{Tr} \left( \mathcal{Z}_A^* \mathcal{L} \mathcal{Z}_B B A^\top \right). \end{aligned}$$

Similarly, the orthogonality constraints read

$$\langle h_i, h_j \rangle_{L^2(\rho)} = \langle \mathcal{Z}_C c_i, \mathcal{Z}_C c_j \rangle_{L^2(\rho)} = \langle c_i, \mathcal{Z}_C^* \mathcal{Z}_C c_j \rangle_{\mathbb{R}^p} = [C^\top \mathcal{Z}_C^* \mathcal{Z}_C C]_{ij} = \delta_{ij}.$$

Note that the operator  $\mathcal{Z}_C$  is equivalent to the operator  $S$  when  $\mathcal{H} = \mathbb{R}^{p_i}$ , and rather then denoting  $\theta$  the elements of  $\mathcal{H}$ , they are denoted by  $c$ . This explains the expression of  $\Sigma_C = \mathbb{E}_{X \sim \rho}[\gamma(X) \otimes \gamma(X)]$  as well as  $L$ . Finally, the fact that the solution is provided by the GSVD follows from the reparameterization of the problem with  $C' = \Sigma_C^{-1/2} C$ , and the application of Courant-Fisher theorem to characterize singular spaces.  $\square$

To ground the discussion, one can check that this generalizes the main text, where we used  $\alpha_i = \beta_i = \kappa(\cdot)^\top \kappa(y_i)$ , together with  $p = p_1 = p_2$ ,  $A = B$ , and we solved in closed form the maximization of (24) with  $f_i = g_i$ .

## C Implementation

This section focuses on the implementation of the principles described in Section 3.

---

### Algorithm 4: Kernel Laplacian algorithm for distance kernel

---

**Data:** Datapoints  $(x_i) \in \mathcal{X}^n$ , a kernel  $k(x, y) = q(\|x - y\|)$ .  
**Result:** Estimate  $(\lambda_i, f_i)$  of the spectral decomposition of  $\mathcal{L}$ .  
Compute  $X = (x_i^\top x_j) \in \mathbb{R}^{p \times n}$ ,  $D = (x_i^\top x_i) \in \mathbb{R}^n$ , and  $N = (\|x_i - x_j\|) \in \mathbb{R}^{p \times n}$   
Initialize  $A = 0 \in \mathbb{R}^{p \times p}$ ; Compute  $B = q(N)q(N)^\top \in \mathbb{R}^{p \times p}$ ;  
**for**  $k \in [n]$  **do**  
  Set  $T_{ij}^{(k)} := (D_k - X_{ik} - X_{jk} + X_{ii}) / \sqrt{(D_k - 2X_{ik} + X_{ii}) \cdot (D_k - 2X_{ik} + X_{ii})}$ ;  
  Update  $A_{ij} \leftarrow A_{ij} + q'(N_{ik})q'(N_{jk})T_{ij}^{(k)}$ ;  
  Solve the generalized eigenvalues problems  $(\lambda_i, (\alpha_{ij})_{j \in [p]})_{i \in [p]} \leftarrow \text{GEVD}(A, B)$ ;  
  Set  $f_i(x) := \sum_{j \in [p]} \alpha_{ij} k(x, x_i)$ .

---

## C.1 Kernel Laplacian

As detailed in Section 3, the spectral decomposition of  $\mathcal{L}$  is linked to the generalized spectral decomposition of  $(L_{\mathcal{H}}, \Sigma_{\mathcal{H}})$  appearing in (15). In other terms, we would like to solve the system  $L_{\mathcal{H}}\theta = \lambda \Sigma_{\mathcal{H}}\theta$ . This system is in the abstract space  $\mathcal{H}$ , it is cast in  $\mathbb{R}^p$  through a “representer” linear embedding  $Z : \mathbb{R}^p \rightarrow \mathcal{H}$  defined for some representer  $(y_i) \in \mathcal{X}^p$  as

$$\theta = Z\alpha := \sum_{i=1}^p \alpha_i \kappa(y_i), \quad \text{with } \alpha = (\alpha_i) \in \mathbb{R}^p. \quad (29)$$

Typically,  $p$  would be much smaller than  $n$  and  $y_i$  could be taken as the  $x_i$  of the training set. This leads to the new system in  $\mathbb{R}^p$  based on the operators

$$[Z^\top L_{\mathcal{H}} Z]_{ij} = \mathbb{E} \left[ \sum_{l \in [d]} \partial_l k(X, y_i) \partial_l k(X, y_j) \right], \quad [Z^\top \Sigma_{\mathcal{H}} Z]_{ij} = \mathbb{E}[k(X, y_i)k(X, y_j)],$$

where  $\partial_l k(x, y)$  has to be understood as the derivative of  $x \mapsto k(x, y)$  with respect to the  $l$ -th coordinate of  $x$ . The expectation can be approximated based on empirical samples. In particular, we shall introduce the computable matrices  $\Sigma, L \in \mathbb{R}^{p \times p}$

$$L_{ij} = \sum_{(m,l) \in [n] \times [d]} \partial_l k(x_m, x_i) \partial_l k(x_m, x_j), \quad \Sigma_{ij} = [K^\top K]_{ij}, \quad (30)$$

where  $K = (k(x_i, x_j))_{ij} \in \mathbb{R}^{n \times p}$ . The spectral decomposition of  $\mathcal{L}$  is estimated through  $(\lambda, SZ\alpha)$  with  $(\lambda, \alpha)$  the generalized eigendecomposition of  $(L, \Sigma)$ . Such a procedure has been proven to learn the spectral decomposition of  $\mathcal{L}$  without suffering the curse of dimension in Cabannes et al. (2021). This is the backbone of their algorithm, whose implementation requires  $O(p^2nd)$  flops to be computed and  $O(pnd)$  in storage. In this paper, we improve both the number of flop and memory cost for usual kernels (e.g. exponential, Gaussian, polynomial kernels). Our improvement is based on the following proposition.

**Proposition 3.** *Assume that  $\mathcal{X}$  is endowed with a scalar product. Given a kernel  $k(x, y) = q(\|x - y\|)$  where  $q : \mathbb{R} \rightarrow \mathbb{R}$ , for  $x, y, z \in \mathcal{X}$ , it holds*

$$\sum_{l \in [d]} \partial_l k(x, y) \partial_l k(x, z) = q'(\|x - y\|) q'(\|x - z\|) \frac{(x - y)^\top (x - z)}{\|x - y\| \|x - z\|}. \quad (31)$$

Similarly for dot-product kernel  $k(x, y) = q(x^\top y)$ , it holds that

$$\sum_{l \in [d]} \partial_l k(x, y) \partial_l k(x, z) = q'(x^\top y) q'(x^\top z) y^\top z. \quad (32)$$

*Proof.* The proof follows from the calculation of  $\langle \nabla_x k(x, y), \nabla_x k(x, z) \rangle$  with the chain rule.  $\square$

Despite its apparent simplicity, Proposition 3 brings the last piece to an efficient algorithm for Laplacian estimation, and more generally the use of derivatives with kernel methods. While naive implementation of Laplacian estimation based on the representer theorem would scale in  $O(n^3d^3)$  in time and  $O(n^2d^2)$  in memory, Proposition 3 allows to reduce the computation to  $O(p^2n + pnd)$  in time and  $O(np)$  in memory. This notably true for the exponential, Gaussian and polynomials kernels, respectively defined as

$$k(x, y) = \exp(-\sigma \|x - y\|), \quad k(x, y) = \exp(-\sigma \|x - y\|^2), \quad k(x, y) = (1 + x^\top y)^d.$$

The implementation consists in computing and storing  $(x_i^\top x_j) \in \mathbb{R}^{n \times p}$  and  $(x_i^\top x_i) \in \mathbb{R}^n$  and using those matrix to compute quantities such as  $g'(\|x_i - x_j\|)$ , so to build the  $p^2$  generalized eigenvalues system  $(A, B)$  and solve it with  $p^3$  flops. Details for dot-product kernels are provided in Algorithm 2 and for translation-invariant kernels in Algorithm 4. Both time and memory cost match exactly the cost of kernel ridge regression. Let us emphasize on the implication of this point: *there is no more computation bottleneck of incorporating Laplacian regularization in (self-, semi-, weakly-) supervised learning when using kernel methods*.

**Graph-Laplacian.** While we focus here on the sub-sampling strategy to estimate  $L$ , similar derivations can be made for graph-Laplacian. We assume that those derivations were already made somewhere, although we were not able to locate them, graph-Laplacian being usually computed in transductive settings that was fashionable in the beginning of this millennium. Our implementation of graph-Laplacian requires to get the generalized eigendecomposition of the system  $(K^\top(I - W)K, K^\top K)$  for  $W = (w_{ij}) \in \mathbb{R}^{n \times n}$  and  $K$  defined in (30). It scales in  $O(n^2d + p^2n)$  regarding the number of flops, since  $n^2d$  is required to compute the weight matrix  $(w_{ij}) \in \mathbb{R}^{n \times n}$  and  $p^2n$  is required to form the reduced  $p^3$  system, and in  $O(n^2)$  in memory which is required to store the weight matrix. Beside being statistically inferior and computationally more expensive, note that graph-Laplacian also introduces an extra hyperparameter, which is the function (and its scale) to compute the weight matrix  $W$ .

## C.2 Deep Learning

The high-level implementation for neural networks is pretty straightforward. Consider  $\varphi_\theta : \mathcal{X} \rightarrow \mathbb{R}^m$  parameterized by a neural network and optimize the loss

$$\min_{\theta} \mathbb{E}_X [F(\varphi_\theta, \varphi_\theta, X)] + \lambda \|\mathbb{E}[\varphi_\theta(X)\varphi_\theta(X)] - I\|^2.$$

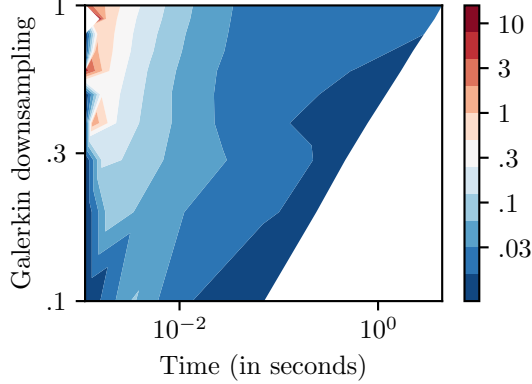


**Figure 5:** Level lines of reconstruction eigenvalues error (in color) in the same setting of Figure 2 as a function of computation time and (Galerkin) downsampling ratio  $p/n$  when using the exponential kernel with  $n \in [10^3]$ . Galerkin method efficiently cuts computation time without compromising on performance even on this small-dimensional example where  $d = 3$ . Indeed, it can even have a regularizer effect that might help performance (the best performance is not achieved for  $p = n$ ).

	Graph-Laplacian	Kernel-Laplacian
Time complexity	$n^2 d + p^2 n$	$p n d + p^2 n$
Memory complexity	$n^2$	$p n$

**Table 1: Computational complexity of graph-Laplacian and kernel-Laplacian.** Not only kernel-Laplacian does not suffer from the curse of dimension, which contrasts with graph-Laplacian, but it does so without requiring extra computations (recall that  $p \leq n$  is taken as a small integer).

If searching for singular eigenfunctions, consider two networks (eventually with shared parameters)  $\varphi_{\theta_1}$  and  $\varphi_{\theta_2}$  and optimize

$$\max_{\theta_1} \min_{\theta_2} \mathbb{E}_X [F(\varphi_{\theta_1}, \varphi_{\theta_2}, X)] - \lambda_1 \|\mathbb{E}[\varphi_{\theta_1}(X)\varphi_{\theta_1}(X)] - I\|^2 + \lambda_2 \|\mathbb{E}[\varphi_{\theta_2}(X)\varphi_{\theta_2}(X)] - I\|^2.$$

Note that the maximum can be replaced by a minimum, it will just yield  $\varphi_{\theta_1}' = -\varphi_{\theta_1}$  but might improve the optimization landscape if  $\theta_1$  and  $\theta_2$  share parameters (e.g. one consider one network that yield output in  $\mathbb{R}^{2m}$  with the first  $m$  output for the left singular functions, the last  $m$  for the right).

Finally, in order to have unbiased stochastic gradient (i.e.  $\mathbb{E}_{\text{mini batch}}[\text{grad}] = \mathbb{E}_{\text{full batch}}[\text{grad}]$ ), one can employ the same trick as for Theorem 1,

$$\|\mathbb{E}_X[A(X)]\|^2 = \mathbb{E}_{X_1, X_2}[A(X_1)A(X_2)],$$

employed with  $A = \varphi(X)\varphi(X)^\top i - I$ . This would allow to get unbiased mini-batch gradient, and eventually reduce the need for big batch that has been required for VICReg (Bardes et al., 2022), since

$$\mathbb{E}_{(X_i)}\|n^{-1} \sum_{i \in [n]} A(X_i)\|^2 \neq \|\mathbb{E}_X[A(X)]\|^2 = 2n^{-1} \mathbb{E}_{(X_i)}[\sum_{i \in [n/2]} A(X_i)A(X_{i+n/2})],$$

meaning that a naive implementation of VCReg does not provide unbiased mini-batch gradient, but there exists a contrastive equivalent that does.

### C.3 Sampling with statistics matching

It should be noted that the fact that the  $(f_i)$  are orthogonal is not required in Theorem 1: one only needs them to be orthogonal to the constant function. As such, one can consider any family of function  $(g_i)_{i \in \mathbb{N}}$  that generates  $L^2(\rho)$  and turn them into  $f_i(x) = g_i(x) - \mathbb{E}_{X \sim \rho}[g_i(X)]$  before using

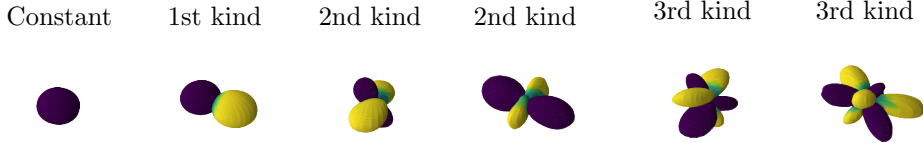


**Figure 6:** Learned spherical harmonics with a neural network. The network is a multi-layer perceptron with 200, 200, 2000, 200 hidden neurons in the four hidden layers, and  $m = 16$  outputs optimized over 5000 batches of size 1000 with the contrastive version of the orthogonal regularizer. The optimizer is stochastic gradient descent with momentum ( $m = 1/2$ ) initialized with a learning rate  $\gamma = 10^{-3}$ , with a scheduler to decrease the learning rate after one third and two third of the learning by a factor 1/3. Principal component analysis was used to disentangle the learned representation and retrieve the different learned eigenspaces and eigenfunctions.

the  $f_i$  as per Theorem 1. In particular, when  $g_i = x^i$ , the objective in (10) assimilates to moments matching. Moments can also be matched with the generating moment function with  $g_i(x) = e^{t_i x}$ , where the  $t_i \in \mathbb{R}$  are chosen so to have

$$(\forall i \in \mathbb{N}, \quad \mathbb{E}_{X \sim \rho}[e^{t_i X}] = \mathbb{E}_{X \sim \mu}[e^{t_i X}]) \quad \Rightarrow \quad \rho = \mu.$$

Since generating moment functions are analytical, such a condition is satisfied if the sequence  $(t_i)$  has an adherence point. We argue that it is even better to condition  $t_i \in \mathbb{R} \cdot \sqrt{-1}$  (where  $\sqrt{-1} = i$  with  $i$  the imaginary number; not to confuse with  $i$  of the index), which corresponds to  $g_i$  being evaluation of the characteristic function. This former function is interesting as it is always defined and takes values in the unit disk of  $\mathbb{C}$  (i.e. its values modulus are bounded by one), which contrast with moments that could takes large values and could lead to badly conditioned gradients when performing backpropagation on deep network architecture to learn the pushforward map  $\psi$  with moment matching. As for the generating moment functions, because characteristic functions are analytical, one does not have to match functions for any  $t \in \mathbb{R}$  but could restrict the matching to take place on a small interval, or on a countable set of well-chosen values for  $t$ . For example, when  $\rho$  is uniform on  $[0, 1]$ ,  $\mathbb{E}[e^{itX}] = -ie^{it}/t$ , and the objective in (10) could be redefined by enforcing a matching on the real part of the characteristic function as  $\int_{t \in \mathbb{R}} \|\mathbb{E}_{Z \sim \nu}[\cos(t\psi(Z))] - \sin(t)/t\|^2 d\mu(t)$ , for some measure  $\mu$  on  $\mathbb{R}$ . Interestingly, when  $\mu$  is the counting measure on  $2\pi\mathbb{N}$ , this is exactly the non-contrastive version of the objective (10) for  $f_i$  the eigenfunctions of the Laplacian  $\mathcal{L} = -\Delta$  and  $c_i = 1$ . Figures 7, 8, 9, 10 plot the loss landscape for the moment generating function matching and the characteristic function matching in well-specified model where the pushforwards in parameterized by two parameters.

## D Experimental details

The eigenvalues reconstruction error Figure 2 was computed by averaging one hundred different runs, the standard deviations of those runs are represented in color-filled regions. The exponential kernel is defined as the translation-invariant kernel associated with  $q(x) = \exp(-\|x\|)$ , the norm on  $\mathcal{X}$  was taken as the norm in  $\mathbb{R}^3$  in which  $\mathbb{S}^2$  is embedded.

More pictures of learned eigenfunctions are offered on Figures 6, 3 and 4.

The sampling transform on Figure 2 was computed using a multi-layer perceptron with 200, 200, 2000 and 200 hidden neurons at the four different layers. It was optimized over mini-batch of size two (the minimum batch size possible) with five thousands such batches, with stochastic gradient descent with momentum ( $m = 1/2$ ) and fixed learning rate ( $\gamma = 10^{-3}$ ).

We found the optimization of the function matching objective to be quite dependent on the different parameters that come into play. In order to better order the loss landscape, Figures 7 and 8 (respectively, 9 and 10) considered stylized setups where the argument distribution is the uniform law on  $[0, 1]$  (respectively, the unit Gaussian  $\mathcal{N}(0, 1)$  on  $\mathbb{R}$ ). The target distribution is the uniform distribution on  $[3, 5]$  (resp.,  $\mathcal{N}(5, 3)$ ), and the pushforward is simply parameterized by  $\psi(x) = ax + b$

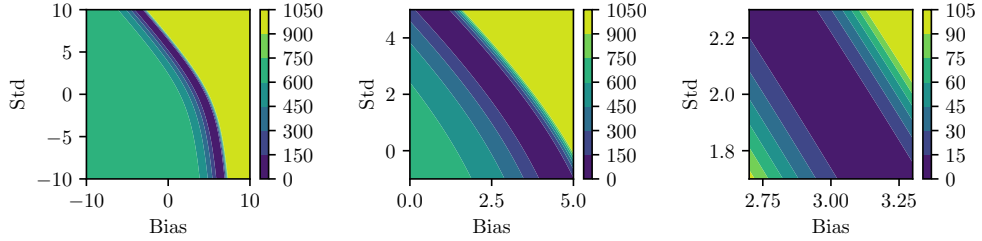


**Figure 7:** Loss landscape for uniform generating moment function matching with  $t \in [100]/1000$ . More exactly, the figure plots the level lines of the function  $\int |\mathbb{E}[e^{(aX+b)t}] - f_{3,5}(t)|^2 T(dt)$  as a function of  $a$  (std.) and  $b$  (bias) when  $T$  is the counting measure on  $[100]/1000$ ,  $Z$  is uniform on  $[0, 1]$  and  $f_{3,5}$  is the generating moment function of the uniform distribution on  $[3, 5]$ . The minimizer is found for  $a = 2, b = 3$  but the loss does not push strongly towards this value.

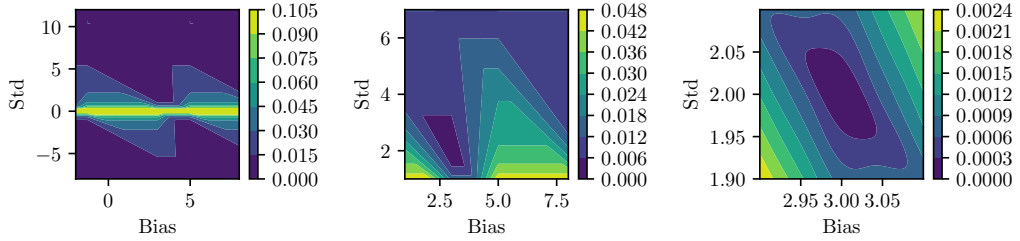


**Figure 8:** Loss landscape for uniform characteristic function matching with  $t \in [10]/10$ . More exactly, the figure plots the level lines of the function  $\int |\mathbb{E}[e^{i(aX+b)t}] - f_{3,5}(t)|^2 T(dt)$  as a function of  $a$  (std.) and  $b$  (bias) when  $T$  is the counting measure on  $[10]/10$ ,  $Z$  is uniform on  $[0, 1]$  and  $f_{3,5}$  is the characteristic function of the uniform distribution on  $[3, 5]$ . Although the loss is not convex, it is relatively well-conditioned around its minimum at  $a = 2, b = 3$ .

for  $a, b \in \mathbb{R}$  to be learned, respectively named standard deviation and bias. Those Figures show how the loss landscape is much better conditioned when considering the characteristic function rather than the moment generating one.

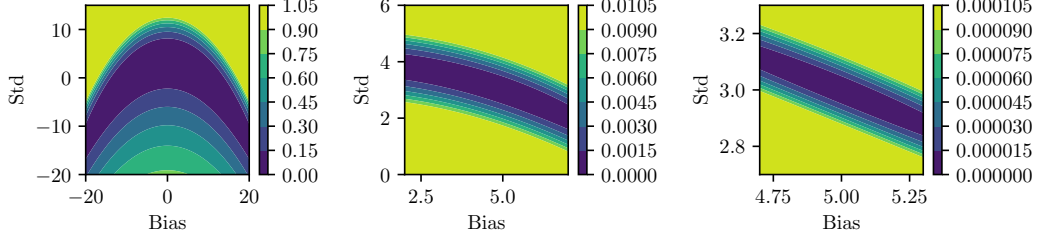


**Figure 9:** Loss landscape for Gaussian generating moment function matching with  $t \in [100]/1000$ . More exactly, the figure plots the level lines of the function  $\int |\mathbb{E}[e^{i(aX+b)t}] - f_{5,3}(t)|^2 T(dt)$  as a function of  $a$  (std.) and  $b$  (bias) when  $T$  is the counting measure on  $[10]/10$ ,  $Z$  is the unit Gaussian  $\mathcal{N}(0, 1)$  and  $f_{5,3}$  is the generating moment function of the Gaussian distribution  $\mathcal{N}(5, 3^2)$ . The minimizer is found for  $a = 3$ ,  $b = 5$  but the loss does not push strongly towards this value.

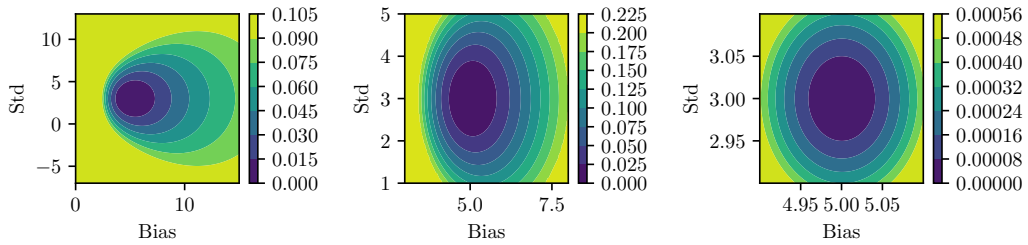


**Figure 10:** Loss landscape for Gaussian characteristic function matching with  $t \in [10]/10$ . More exactly, the figure plots the level lines of the function  $\int |\mathbb{E}[e^{i(aX+b)t}] - f_{5,3}(t)|^2 T(dt)$  as a function of  $a$  (std.) and  $b$  (bias) when  $T$  is the counting measure on  $[10]/10$ ,  $Z$  is the unit Gaussian  $\mathcal{N}(0, 1)$ , and  $f_{5,3}$  is the characteristic function of the Gaussian distribution  $\mathcal{N}(5, 3^2)$ . The loss is really well-conditioned, it even seems to be convex.